Knee Point Identification Based Decision Making for Parameter Selection in Network Designing

Hainan Zhang, Jianhou Gan, Juxiang Zhou, Wei Gao

***Abstract*—In graph-based modelled networks, connectivity and toughness are two types of parameters to measure the robustness of graphs (corresponding networks), and recent studies have shown that these variables are explicitly associated with the existence of $\mathcal{H}$-factors in specific settings, where the latter is inner connected to the feasibility of data transmission in networks. However, the previous contributions presented in the form of several surfaces of connectivity and toughness (isolated toughness or sun toughness) lead to a "choice dilemma" for decision-makers in the network designing stage. In this work, to overcome this problem, we propose a new approach in terms of knee point identification to determine the best combination of connectivity and toughness related parameters. The family of knee points on curves are implemented which vary with respect to m or k.**

***Index Terms*—network, connectivity, toughness, knee point identification (KPI), decision making (DM)**

I. Introduction

Among many network models, the graph model (sites and channels are modelled by vertices and edges respectively) can effectively describe the topology of the network. Throughout this paper, only simple, undirected and finite graph G (corresponds to a network) with vertex set $V(G)$ and edge set $E(G)$ is discussed. Denote $\kappa(G)$ as the connectivity of G which implies how many vertices are deleted at least to make G disconnected. Toughness and its related variables are celebrated graph-based parameters in networks to measure the vulnerability of networks, which are summarized by Gao et al. [1] and presented in Tab. I. It is noteworthy that if G is a complete graph, then $t(G) = \tau(G) = I(G) = I'(G) = s(G) = s'(G) = +\infty$ since there is no vertex subset meeting the restriction.

Let $\mathcal{H}$ be the set of connected graphs. An $\mathcal{H}$-factor of graph G is a spanning subgraph such that each component is isomorphic to an element of $\mathcal{H}$. A graph G is a $(\mathcal{H}, k)$-factor critical graph (resp. $(\mathcal{H}, m)$-factor deleted graph) if removing any k vertices (resp. m edges) from G, the resulting subgraph still admits $\mathcal{H}$-factor. For instance, if $\mathcal{H}$ is the set of paths with the length at least 3, then we denote $\mathcal{H} = P_{\geq 3}$.

Several recent contributions (cf. Gao et al. [1], [9] and [10]) studied the tight bounds of toughness related parameters (variables) for the existence of $\mathcal{H}$-factor, and it is found that there are massive influences among multiple parameters. For example, the combination of toughness and connectivity conditions, if the toughness condition is enhanced, the connectivity condition is weakened; conversely, if the connectivity condition is increased, the toughness condition is weakened. This reveals that the multi-parameter tight bound of $\mathcal{H}$-factor is imperative to treat these graph-based variables as a dynamic system, and the change of one will cause the synergistic changes of other variables. In order to characterize the dynamic changing relationship between various parameters, they look at this problem from the perspective of high-dimensional space, i.e., express the combination of various parameters as a vector in high-dimensional space, and then multi-dimensional surfaces are utilized to describe such implicit correlation. Gao et al. [1], [9] and [10] studied the parametric conditions for the existence of $\mathcal{H}$-factors in specific settings, where the surfaces of the combination of parameters such as toughness, isolated toughness, binding number and connectivity are obtained.

The yardstick multi-objective optimization problem (MOP) can be formulated as

$$\min \mathbf{F}(\mathbf{x}) = (f_1(\mathbf{x}), \cdots, f_r(\mathbf{x}))^T$$
$$\text{s.t.}\, \mathbf{x} \in \Omega$$

where $\mathbf{x} = (x_1, \cdots, x_d)^T$ is a decision vector (regarded as a candidate solution of MOP) and Ω is a decision space. If $r = 2$, then MOP is called a bi-objective optimization. For two solutions $\mathbf{x}^1, \mathbf{x}^2 \in \Omega$, we say $\mathbf{x}^1$ dominates $\mathbf{x}^2$ (denoted by $\mathbf{x}^1 \preceq \mathbf{x}^2$) if and only if $f_i(\mathbf{x}^1) \leq f_i(\mathbf{x}^2)$ for all $i \in \{1, \cdots, r\}$ and $f_i(\mathbf{x}^1) < f_i(\mathbf{x}^2)$ for at least one $i \in \{1, \cdots, r\}$. A solution $\mathbf{x} \in \Omega$ is Pareto optimal if there isn't exist a solution $\mathbf{x}' \in \Omega$ such that $\mathbf{x}' \preceq \mathbf{x}$, the set of all Pareto optimal solutions is called the Pareto set (PS) and the set of their corresponding values $\{\mathbf{F}(\mathbf{x}) | \mathbf{x} \in \text{PS}\}$ is called the Pareto front (PF).

As a follow-up to Gao et al. [1], [9] and [10], this paper considers the selection of multiple parameters in the network construction process from the perspective of a decision maker. From the perspective of MOP, the last two dimensions of the given surfaces are regarded as the PF obtained by bi-objective optimization, and a novel knee point identification (KPI) approach is designed for this specific application problem to obtain the knee points of the corresponding curves (cross-sections).

The difference between the KPI approach presented in this article and the KPI algorithms in extant MOP algorithms is reflected in the following two key points:

(1) Since κ can be infinitely large, the corresponding PF involves infinite points. In this case, there is theoretically no extreme point, and hence the traditional KPI methods cannot be applied to the application scenarios in this article.

Manuscript received September 27, 2023; revised January 24, 2024. This work has been partially supported by National Science Foundation of China (No. 12161094).

J. Gan is a professor of Key Laboratory of Educational Information for Nationalities, Yunnan Normal University, Kunming 650500, China, e-mail: ganjh@ynnu.edu.cn.

H. Zhang is a postgraduate student of School of Information, Yunnan Normal University, Kunming 650500, China, e-mail: 2123100065@ynnu.edu.cn.

J. Zhou is a professor of Key Laboratory of Educational Information for Nationalities, Yunnan Normal University, Kunming 650500, China, e-mail: zhoujuxiang@ynnu.edu.cn.

W. Gao is a professor of the School of Information, Yunnan Normal University, Kunming, 650000, China, e-mail: gaowei@ynnu.edu.cn.

TABLE I
PARAMETERS IN TOUGHNESS FAMILY [1].

parameter	notation	formulation	restriction	reference
toughness	$t(G)$	$\min\left\{\frac{\lvert S\rvert}{\omega(G-S)}\right\}$	$S\subset V(G)$ and $\omega(G-S)\ge 2$	Chvátal [2]
variant of toughness	$\tau(G)$	$\min\left\{\frac{\lvert S\rvert}{\omega(G-S)-1}\right\}$	$S\subset V(G)$ and $\omega(G-S)\ge 2$	Enomoto et al. [3]
isolated toughness	$I(G)$	$\min\left\{\frac{\lvert S\rvert}{i(G-S)}\right\}$	$S\subset V(G)$ and $i(G-S)\ge 2$	Yang et al. [4]
variant of isolated toughness	$I'(G)$	$\min\left\{\frac{\lvert S\rvert}{i(G-S)-1}\right\}$	$S\subset V(G)$ and $i(G-S)\ge 2$	Ma and Liu [5]
sun toughness	$s(G)$	$\min\left\{\frac{\lvert S\rvert}{sun(G-S)}\right\}$	$S\subset V(G)$ and $sun(G-S)\ge 2$	Zhou et al. [6]
variant of sun toughness	$s'(G)$	$\min\left\{\frac{\lvert S\rvert}{sun(G-S)-1}\right\}$	$S\subset V(G)$ and $sun(G-S)\ge 2$	Zhu et al. [7]
binding number	$bind(G)$	$\min\left\{\frac{\lvert N_G(X)\rvert}{\lvert X\rvert}\right\}$	$\emptyset\ne X\subseteq V(G)$ and $N_G(X)\ne V(G)$	Woodall [8]

(2) Since the value of κ varies with the value of m or k, there are infinitely PFs (each PF corresponding to a cross-section of the given surface). This setting is beyond the consideration of traditional MOP problems.

Overall, based on the above two facts, the KPI problem discussed in this article is much more complex than traditional KPI problems in the corresponding MOP settings, and therefore, a new parameter ε is introduced for this problem.

The remainder of this article is organized as follows. We elaborate on the contributions in Gao et al. [1], [9] and [10] in the next section, and then the motivation for this work is stated in the third section. After that, we propose our main KPI approach to determine the knee points of corresponding cross-sections. As supplementary results, we added a remark section. In this remark, we assume that dimensionality reduction operator is utilized to map high-dimensional graph data to real numbers, so that the functions g and f can be represented on a two-dimensional plane. On this basis, we consider the embedding problem of p, the restrained embeddings are proposed, as well as in the high dimensional space setting. Finally, the future study topics are discussed.

II. RELATED WORKS

What Gao et al. [1], [9] and [10] have in common is to present multi-parameter (multi-variable) conditions for the existence of $\mathcal{H}$-factor in vertex removing or edge deleting settings. Hence, before starting a formal motivation, we must elaborate on the main results of these three papers. In what follows, let $m,k\in\mathbb{N}$, and κ be the lower bound of connectivity of G which is the function of m or k (i.e., $\kappa\ge m+1$ in factor deleted graph setting, and $\kappa\ge k+1$ in factor critical graph setting).

Let $I^{tight}_{(\ge 3,m)-FD}$ (resp. $I^{*,tight}_{(\ge 3,m)-FD}$) be the sharp $I(G)$ (resp. $I'(G)$) bound for a graph G with $\kappa(G)\ge\kappa$ to be $(P_{\ge 3},m)$-factor deleted, where $I^{tight}_{(\ge 3,m)-FD}$ (resp. $I^{*,tight}_{(\ge 3,m)-FD}$) is a function of m and κ. We call $(m,\kappa,I^{tight}_{(\ge 3,m)-FD})$ (resp. $(m,\kappa,I^{*,tight}_{(\ge 3,m)-FD})$) as "isolated toughness $(P_{\ge 3},m)$ factor deleted surface" (resp. "isolated toughness variant $(P_{\ge 3},m)$ factor deleted surface"), in short, IT-$(P_{\ge 3},m)$-FDS (resp. ITV-$(P_{\ge 3},m)$-FDS). Gao et al. [9] determined that the exact expression of IT-$(P_{\ge 3},m)$-FDS and ITV-$(P_{\ge 3},m)$-FDS are $(m,\kappa,\frac{3\kappa+1-m}{2\kappa+1-m})$ and $(m,\kappa,\frac{3\kappa+1-m}{2\kappa-m})$, respectively. The functions of curves induced by the last two dimensional parameters of the above two surfaces are denoted by f^1_m and f^2_m respectively.

Let $t^{tight}_{(\ge 3,m)-FD}$ (resp. $t^{*,tight}_{(\ge 3,m)-FD}$) be the sharp $t(G)$ (resp. $\tau(G)$) bound for a graph G with $\kappa(G)\ge\kappa$ to be $(P_{\ge 3},m)$-factor deleted, where $t^{tight}_{(\ge 3,m)-FD}$ (resp. $t^{*,tight}_{(\ge 3,m)-FD}$) is a function of m and κ. We call $(m,\kappa,t^{tight}_{(\ge 3,m)-FD})$ (resp. $(m,\kappa,t^{*,tight}_{(\ge 3,m)-FD})$) as "toughness $(P_{\ge 3},m)$ factor deleted surface" (resp. "toughness variant $(P_{\ge 3},m)$ factor deleted surface"), in short, TP3mFDS (resp. TVP3mFDS). One of the main results in Gao et al. [10] determined that the exact expression of TP3mFDS and TVP3mFDS are $(m,\kappa,\frac{\kappa}{2\kappa-m+1})$ and $(m,\kappa,\frac{\kappa}{2\kappa-m})$, respectively. The functions of curves induced by the last two dimensional parameters of the above two surfaces are denoted by f^3_m and f^4_m respectively.

Let $I^{tight}_{(\ge 3,k)-FC}$ (resp. $I^{*,tight}_{(\ge 3,k)-FC}$) be the sharp $I(G)$ (resp. $I'(G)$) bound for a graph G with $\kappa(G)\ge\kappa$ to be $(P_{\ge 3},k)$-factor critical, where $I^{tight}_{(\ge 3,k)-FC}$ (resp. $I^{*,tight}_{(\ge 3,k)-FC}$) is a function of m and κ. We call $(k,\kappa,I^{tight}_{(\ge 3,k)-FC})$ (resp. $(k,\kappa,I^{*,tight}_{(\ge 3,k)-FC})$) as "isolated toughness $(P_{\ge 3},k)$ factor critical surface" (resp. "isolated toughness variant $(P_{\ge 3},k)$ factor critical surface"), in short, ITP3kFCS (resp. ITVP3kFCS). Gao et al. [10] determined that the exact expression of ITP3kFCS and ITVP3kFCS are $(k,\kappa,\frac{3\kappa-2k+1}{2\kappa-2k+1})$ and $(k,\kappa,\frac{3\kappa-2k+1}{2\kappa-2k})$, respectively. The functions of curves induced by the last two dimensional parameters of these two surfaces are denoted by f^5_k and f^6_k respectively.

Gao et al. [1] studied the existence of $\mathcal{H}$-factor whose necessary and sufficient condition can be stated by

$$i(G-S)\le q|S|, \tag{1}$$

where $q\ge 1$ is a half-integer (i.e., $q\in\{1,\frac{3}{2},2,\frac{5}{2},\cdots\}$), $S\subseteq V(G)$ and $i(G-S)$ is the number of isolated vertices in $G-S$. Let $\mathcal{P}$ be a specific parameter described in Tab. I and $\mathcal{P}^{tight}_{(\mathcal{H},k)-FC}$ be a tight $\mathcal{P}$ bound (which is a function of q, k and κ) for a graph G to be $(\mathcal{H},k)$-factor critical. The 4-dimensional surface $(q,k,\kappa,\mathcal{P}^{tight}_{(\mathcal{H},k)-FC})$ implies that G is a $(\mathcal{H},k)$-factor critical graph if $\kappa(G)\ge\kappa$ and $\mathcal{P}>\mathcal{P}^{tight}_{(\mathcal{H},k)-FC}$, where the existence of $\mathcal{H}$-factor is characterized by (1). The first main theorem in Gao et al. [1] argued that under the mild condition on $\kappa-k$ and qk, the above 4-dimensional surface can be determined by $(q,k,\kappa,\frac{\kappa}{\Theta})$ if $\mathcal{P}(G)\in\{t(G),s(G),I(G),bind(G)\}$ and by $(q,k,\kappa,\frac{\kappa}{\Theta-1})$ if $\mathcal{P}(G)\in\{\tau(G),s'(G),I'(G)\}$, where

$$\Theta(q,k,\kappa)=\begin{cases}\lceil q(\kappa-k)\rceil, & \text{if } q(\kappa-k) \text{ is not an integer,}\\ q(\kappa-k)+1, & \text{if } q(\kappa-k) \text{ is an integer.}\end{cases}$$

The functions of curves induced by the last two dimensional parameters of the above two surfaces are denoted by f_k^7 and f_k^8 respectively.

Let $\mathcal{P}^{tight}_{(\mathcal{H},m)-FD}$ be a tight $\mathcal{P}$ bound (which is a function of q, m and κ) for a graph G to be $(\mathcal{H}, m)$-factor deleted. The 4-dimensional surface $(q, m, \kappa, \mathcal{P}^{tight}_{(\mathcal{H},m)-FD})$ reveals that G is a $(\mathcal{H}, m)$-factor deleted graph if $\kappa(G) \geq \kappa$ and $\mathcal{P} > \mathcal{P}^{tight}_{(\mathcal{H},m)-FD}$, where the existence of $\mathcal{H}$-factor is characterized by (1). The second main result in Gao et al. [1] stated that under the mild condition on q, m and κ, this 4-dimensional surface can be formulated by

(1) $(q, m, \kappa, \frac{\kappa}{\Gamma - m})$ if $\mathcal{P}(G) = t(G)$;
(2) $(q, m, \kappa, \frac{\kappa}{\Gamma - m - 1})$ if $\mathcal{P}(G) = \tau(G)$;
(3) $(q, m, \kappa, \frac{\kappa + \lfloor \frac{m}{2} \rfloor}{\Gamma - \lceil \frac{m}{2} \rceil})$ if $\mathcal{P}(G) = s(G)$;
(4) $(q, m, \kappa, \frac{\kappa + \lceil \frac{m}{2} \rfloor}{\Gamma - \lceil \frac{m}{2} \rceil - 1})$ if $\mathcal{P}(G) = s'(G)$;
(5) $(q, m, \kappa, \frac{\kappa + m}{\Gamma - m})$ if $\mathcal{P}(G) = I(G)$;
(6) $(q, m, \kappa, \frac{\kappa + m}{\Gamma - m - 1})$ if $\mathcal{P}(G) = I'(G)$;
(7) $(q, m, \kappa, \frac{\kappa + 2m}{\Gamma})$ if $\mathcal{P}(G) = bind(G)$.

Here,

$$\Gamma(q, \kappa) = \begin{cases} \lceil q\kappa \rceil, & \text{if } q\kappa \text{ is not an integer,} \\ q\kappa + 1, & \text{if } q\kappa \text{ is an integer.} \end{cases}$$

The functions of curves induced by the last two dimensional parameters of the above surfaces are denoted by f_m^9 and f_m^{15} respectively.

III. Motivation

The toughness-related variables in Tab. I are salient parameters to measure the vulnerability of the network. The larger the parameter value, the stronger the corresponding network. An extreme idea is to directly construct a complete graph network, that is, any two vertices are connected by edges, so that the corresponding parameter value will reach the maximum value. However, due to the excessive construction cost, such a fully connected network will not be adopted in reality. The parameter bound obtained in [1], [9] and [10] theoretically yields the balance point for network construction. For example, consider the first surface $(m, \kappa, \frac{3\kappa+1-m}{2\kappa+1-m})$ in literature Gao et al. [9], the last parameter $\frac{3\kappa+1-m}{2\kappa+1-m}$ characters the tight isolated toughness bound for data transmission by path when network congestion or attack (the channel corresponding to m edges is unavailable). Therefore, according to this conclusion, it only needs to design the network with connectivity not less than $\kappa(G)$, its isolated toughness is greater than $\frac{3\kappa+1-m}{2\kappa+1-m}$, and there is no need to construct a complete graph network with a heavy financial burden.

However, [1], [9] and [10] only gave the specific form of the surface from a theoretical point of view, but didn't analyze the practical problems from the point of view of network applications. We instantiate $(m, \kappa, \frac{3\kappa+1-m}{2\kappa+1-m})$ for actual problems, where a cross-section of the last two parameters is given by fixing m, and infinite points are drawn in the corresponding curve since $\kappa \geq m + 1$ is an integer. That is, take κ equal to $m+1$, $m+2$, $\cdots$, then we get $(m+1, \frac{2m+4}{m+3})$, $(m + 2, \frac{2m+7}{m+5})$, $\cdots$. We verify that as the value of κ increases, the value of $\frac{3\kappa+1-m}{2\kappa+1-m}$ decreases. Hence, there is a balance between connectivity and isolated toughness, where an increase in one leads to a decrease in the other.

For network designers, it is imperative to choose a combination of connectivity and toughness related variables as a reference for building a network. However, since there are infinitely pairs of parameters, this leads to a choice barrier for network designers (see Li et al. [11], Purshouse et al. [12], Lai et al. [13], Bhattacharjee et al. [14] and He et al. [15], [16], [17], [18] for such problems in MOP settings). How to determine a pair of optimal combinations from infinite pairs of parameter combinations has become a challenging problem.

Notably, there are 15 surfaces in [1], [9] and [10], which generate 15 families of curves from the last two parameters of each surface. These curves from 15 families describe the balanced relationship between connectivity and toughness-related parameters in specific $\mathcal{H}$-factor settings from different $\mathcal{P}(G)$ perspectives. Studying the equilibrium point of each curve can allow the network designer to find the optimal balance position and avoid the choice dilemma.

Before presenting the specific method, we need to clarify the following two statements:

(1) The values of m and k to some extent indicate the requirements to build a network, and their values are predetermined under specific engineering demands. But from a theoretical perspective, it is still necessary to consider them as variables.
(2) To facilitate the characterization of curves, we treat all variables as continuous variables.

IV. KPI based implementation

The main idea of this paper comes from MOP, where each curve is regarded as a PF in a bi-objective optimization problem, and we propose a knee point identification approach to determine the knee point for each curve.

In MOP setting, the knee point is the point on the Pareto front with maximum effectiveness, near which satisfying a small increase in the value of one objective will cause a large recession in at least one other objective [19]. And global knee point can be denoted as

$$\mathbf{x}_{kp} = \arg\max_{\mathbf{x} \in \Omega} Dis(\mathbf{F}(\mathbf{x}), \mathbb{H}), \tag{2}$$

where $\mathbb{H}$ is a hyperplane on the objective space, which generally consists of extreme points on the objective space, and $Dis(\cdot)$ is the Euclidean distance from the feasible solution $\mathbf{x}$ to $\mathbb{H}$. As shown in Fig. 1, the point with maximum $Dis(\cdot)$ from the $\mathbb{H}$ is considered as the global knee point.

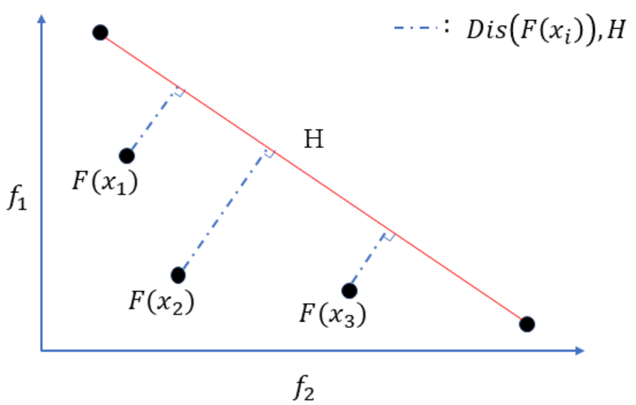

Fig. 1. Selection of global knee point

Unlike traditional KPI, in this work, we focus on one of the objective values $f_m^i(\mathbf{x}) \in [\mathbf{C}, +\infty]$, so we have to determine the extreme points first. The KPI in this work is not to find one or a set of knee points only on a curve, but to find the dynamic relationship between κ and m (resp. k) under certain qualifying conditions on a family of curves about m (resp. k). For the above curves $f_m^n(x)$ in 15 families where $n \in [1, 15] - \{5, 6, 7, 8\}$ (resp. $f_k^n(x)$ where $n \in \{5, 6, 7, 8\}$), we assume that Ω and the objective space are the same, i.e., the global knee point is a point on $f_m^n(x)$ (resp. $f_k^n(x)$). All curves in this paper are monotone with a lower bound, which means that

$$\lim_{x \to \infty} f_m^n(x) = C$$

or

$$\lim_{x \to \infty} f_k^n(x) = C$$

where C is a constant. In order to find the extreme points in the direction of the x-axis, we assume that for $\forall \varepsilon \geq 0$, there exists a positive number M on its domain of definition $[m+1, +\infty]$ (resp. $[k+1, +\infty]$), and when x is greater than M there is $|f(x) - C| < \varepsilon$. And then we take the first positive integer $(x_{e2}, f_m^n(x_{e2}))$ (resp. $(x_{e2}, f_k^n(x_{e2}))$) that satisfies the requirement as an extreme point in the x-axis direction and $x_{e1} = m + 1$ (resp. $x_{e1} = k + 1$). We pick different values of error ε to determine the extreme points. Take curve $f_m^1 = \frac{3\kappa+1-m}{2\kappa+1-m}$ as an example, where $\kappa \geq m + 1$, $m = 2$ and ε = 0.01. As shown in Fig. 2, their extreme points are indicated by black circles and pentagrams, respectively. It is worth noting that $f_m^1(x) = \frac{3}{2}$ when $m = 1$.

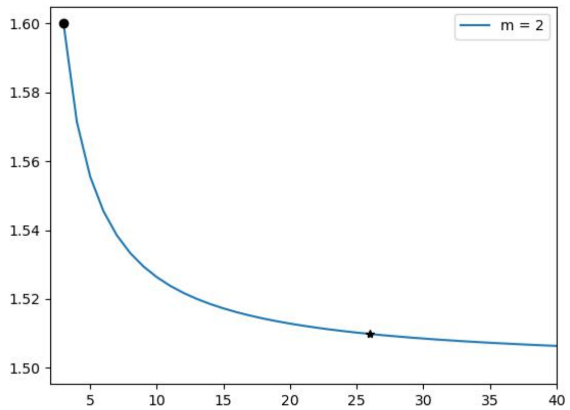

Fig. 2. Selection of extreme points

In order to minimize the selection pressure for the decision maker, we choose different ε to give the relationship between m (resp. k) and κ for the global knee point of the above curves in 15 families. In this paper, we set $\varepsilon = 0.01$, 0.005 and 0.001, and $m \in [1, 100]$ (resp. $k \in [1, 100]$) to select 100 global knee points. Then m (resp. k) and κ are found by polynomial fitting, and the specific results are shown in Tab. II and Tab. III.

For a longitudinal comparison of the first six curves, we find that the slope of $f_m(\kappa)$ (resp. $f_k(\kappa)$) increases as ε increases. However, by comparing horizontally, we find that the coefficient of m (resp. k) affects $f_m(\kappa)$ (resp. $f_k(\kappa)$) to a large extent.

Fig. 3-8 illustrate the image of the curves and m (resp. k) is taken from 1 to 9, where the black dots and pentagrams

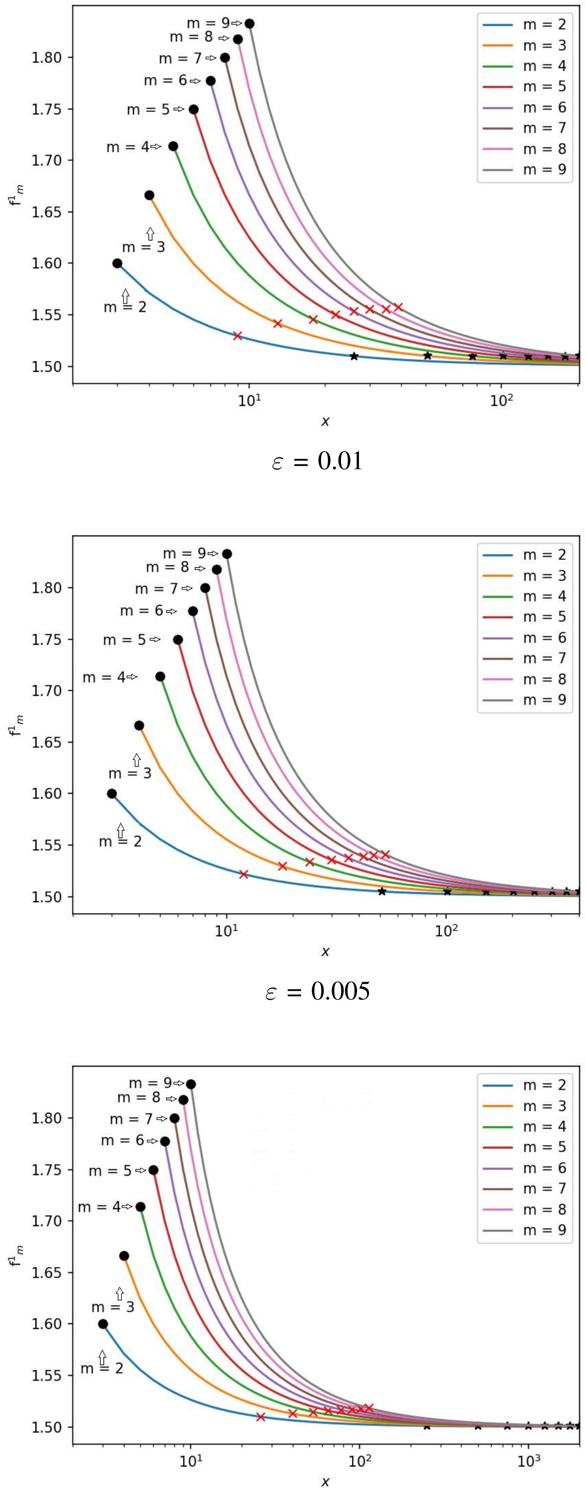

Fig. 3. The curve f_m^1 of $m \in [1, 9]$, where the black dots and pentagrams represent the extreme points, and the red $\times$ represents the global knee point of the function.

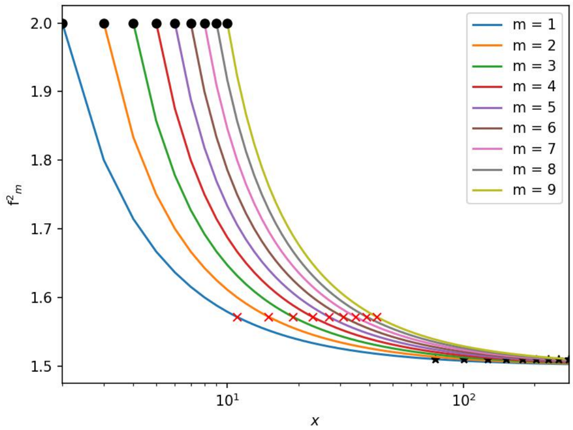

ε = 0.01

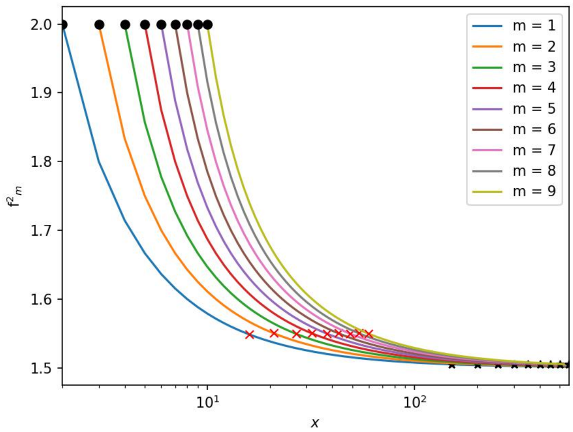

ε = 0.005

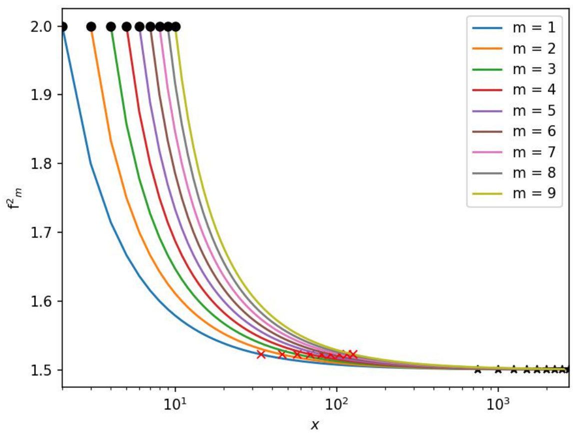

ε = 0.001

Fig. 4. The curve f_m^2 of $m \in [1, 9]$, where the black dots and pentagrams represent the extreme points, and the red $\times$ represents the global knee point of the function. The curves in the figure from left to right are $m = 1$ to 9 respectively.

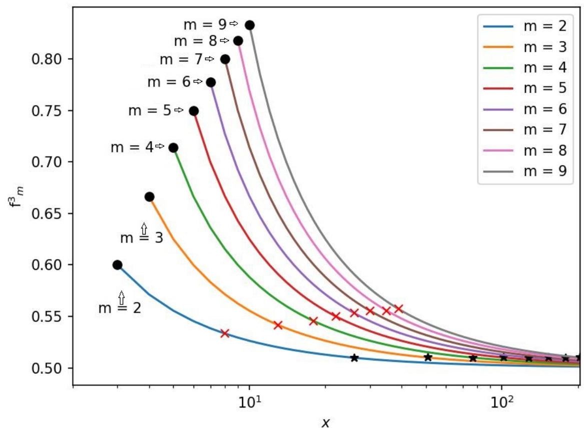

ε = 0.01

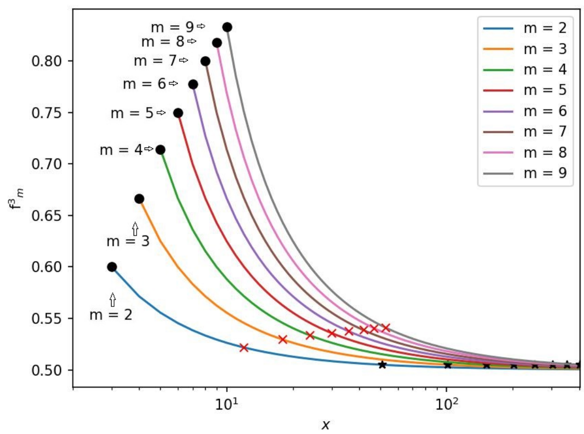

ε = 0.005

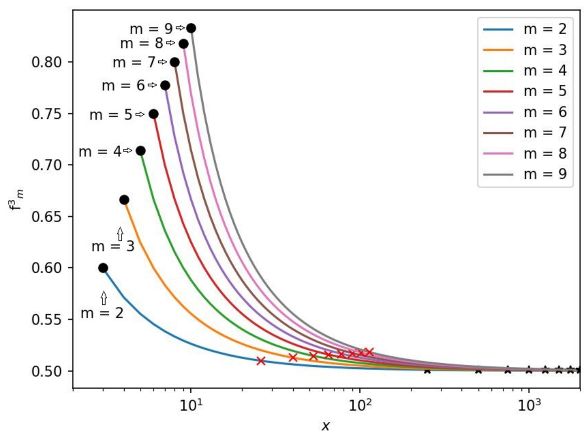

ε = 0.001

Fig. 5. The curve f_m^3 of $m \in [1, 9]$, where the black dots and pentagrams represent the extreme points, and the red $\times$ represents the global knee point of the function.

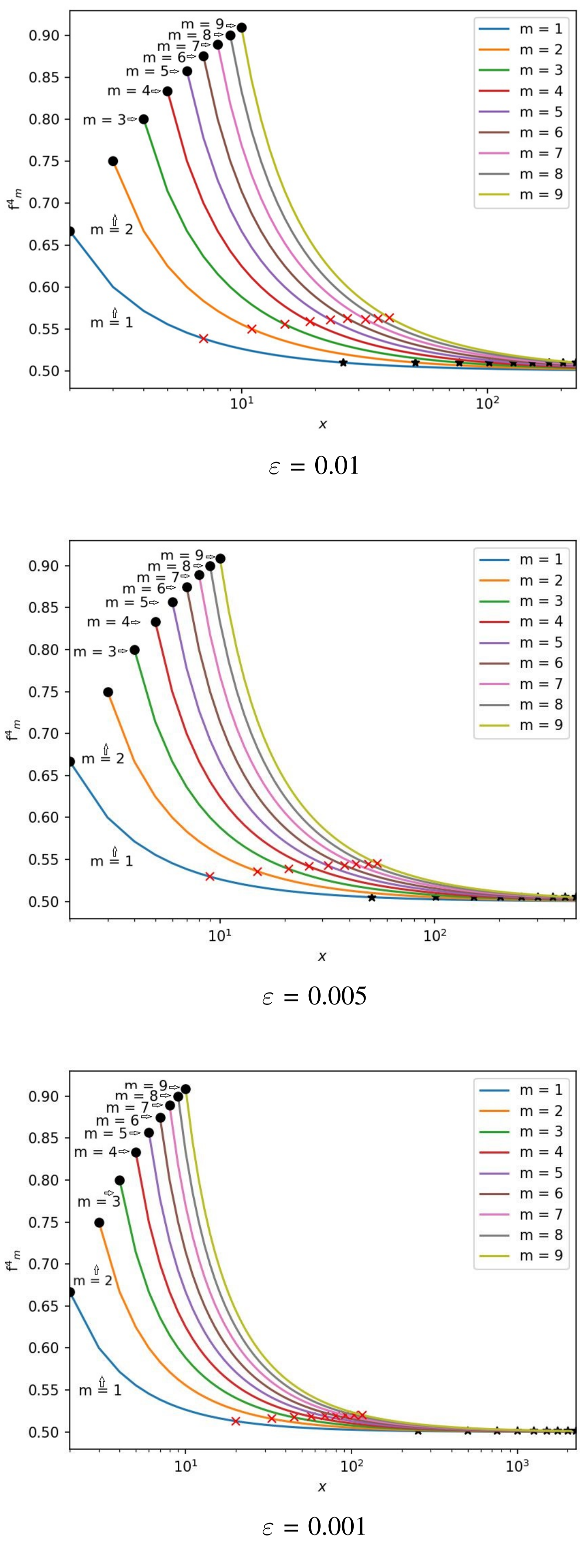

Fig. 6. The curve f_m^4 of $m \in [1, 9]$, where the black dots and pentagrams represent the extreme points, and the red $\times$ represents the global knee point of the function.

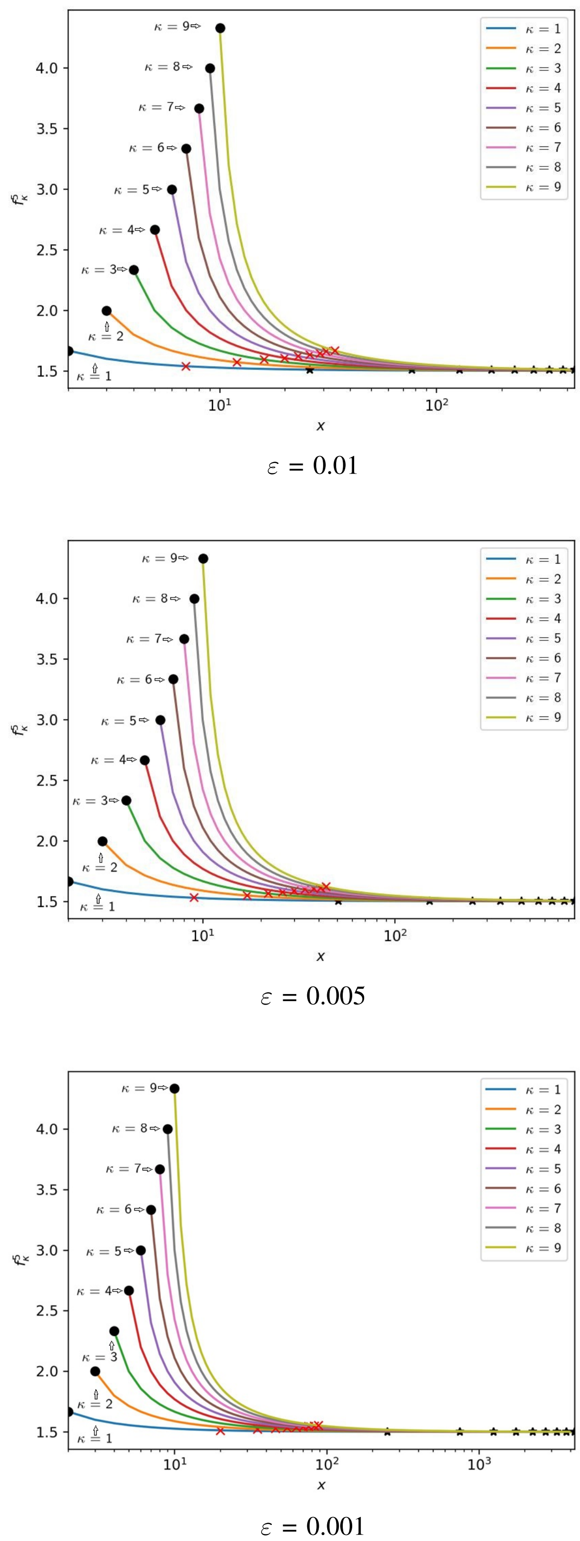

Fig. 7. The curve f_k^5 of $k \in [1, 9]$, where the black dots and pentagrams represent the extreme points, and the red $\times$ represents the global knee point of the function.

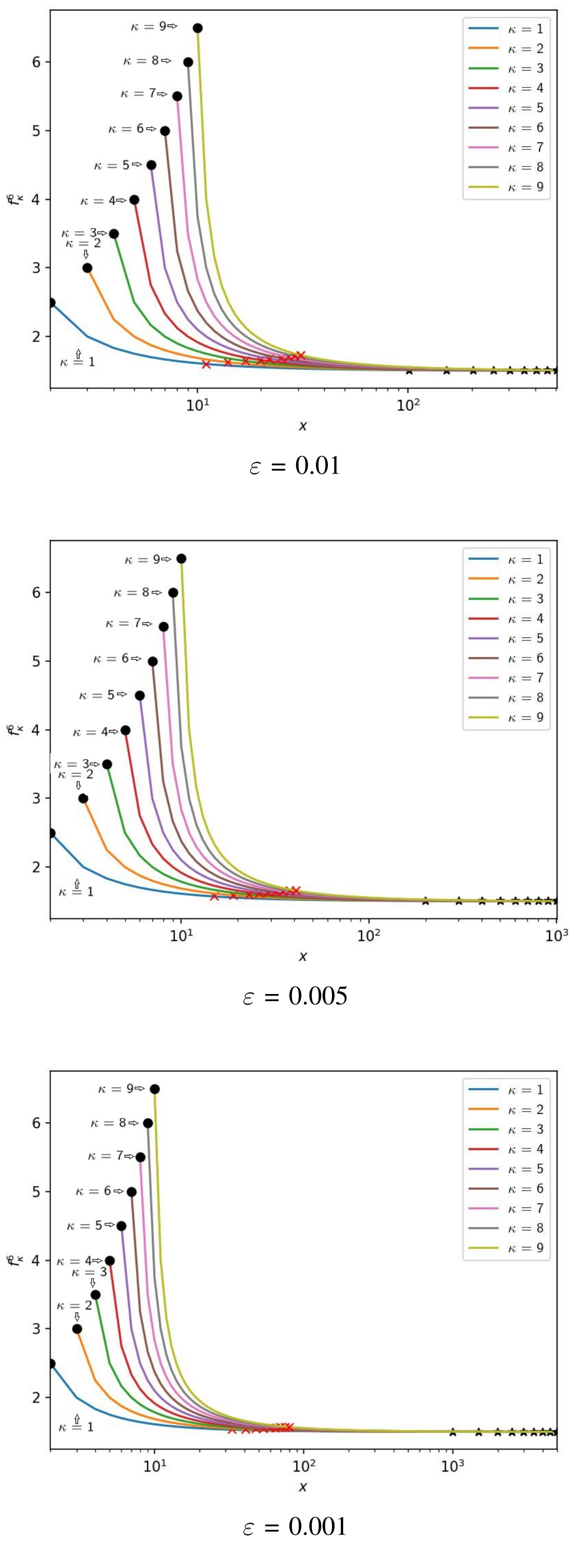

Fig. 8. The curve f_k^6 of $k \in [1, 9]$, where the black dots and pentagrams represent the extreme points, and the red $\times$ represents the global knee point of the function.

TABLE II
THE m (RESP. k) AND κ FUNCTIONALS OF $f_m^1, \cdots, f_k^6$ FOR DIFFERENT ε CASES.

f_m^n (resp. f_k^n)	ε	$f^n(m)$ (resp. $f^n(k)$)
$f_m^1 = \frac{3\kappa+1-m}{2\kappa+1-m}$	0.01	$\kappa = 4.042m + 2.413$
	0.005	$\kappa = 5.511m + 3.519$
	0.001	$\kappa = 11.71m + 8.491$
$f_m^2 = \frac{3\kappa+1-m}{2\kappa-m}$	0.01	$\kappa = 4.036m + 7.025$
	0.005	$\kappa = 5.5m + 10.25$
	0.001	$\kappa = 11.68m + 22.331$
$f_m^3 = \frac{\kappa}{2\kappa-m+1}$	0.01	$\kappa = 4.043m + 2.372$
	0.005	$\kappa = 5.511m + 3.519$
	0.001	$\kappa = 11.71m + 8.491$
$f_m^4 = \frac{\kappa}{2\kappa-m}$	0.01	$\kappa = 4.038m + 3.321$
	0.005	$\kappa = 5.502m + 4.609$
	0.001	$\kappa = 11.69m + 10.57$
$f_k^5 = \frac{3\kappa-2k+1}{2\kappa-2k+1}$	0.01	$\kappa = 1.695k + 22.24$
	0.005	$\kappa = 1.985k + 31.48$
	0.001	$\kappa = 3.202k + 71.06$
$f_k^6 = \frac{3\kappa-2k+1}{2\kappa-2k}$	0.01	$\kappa = 1.553k + 20.15$
	0.005	$\kappa = 1.779k + 28.71$
	0.001	$\kappa = 2.744k + 64.19$

represent the extreme points, and the red $\times$ represents the global knee point of the function. (If there is no curve with $m = 1$ (resp. $k = 1$) in the images, it means that the function f_m^n (resp. f_k^n) is a straight line parallel to the x-axis at $m = 1$ (resp. $k = 1$).) As ε decreases, the distance between the two extreme points will consequently become larger, which will undoubtedly affect the position of the knee point. Fig. 9 demonstrates the location of the knee points for different extreme point selections, from top to bottom ε is 0.01, 0.005 and 0.001.

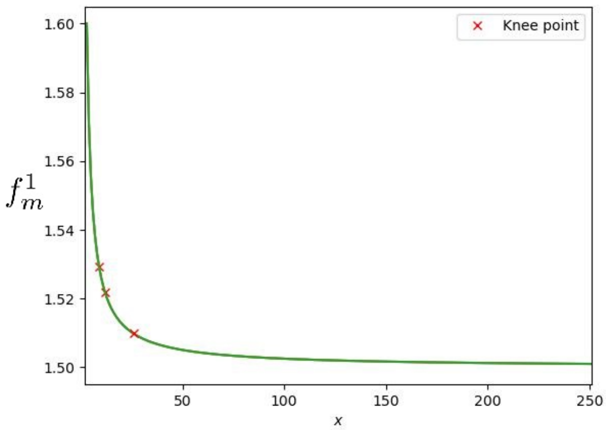

Fig. 9. Different Knee Points

Fig. 10 shows the linear relationship between κ and m (or, k for f^5 and f^6) for curves $f_m^1, \cdots, f_k^6$ when ε = 0.01. It is easy to see that when the coefficient of m (resp. k) in the curves is 1, the sampled points and the fitted curves fit well, but when the coefficient of m (resp. k) is 2, there is a certain degree of deviation.

Tab. III shows, for curves $f_k^7, \cdots, f_m^{15}$, the linear relationship between m (or k for f^7 and f^8) and κ for different q and ε. Fig. 13-21 show curves $f_k^7, \cdots, f_m^{15}$, where the black pentagrams and dots represent the extreme points at each end, and the red $\times$ represents the global knee points. In order to showcase the knee points clearly, only up to 500 is shown on the x-axis, so it is possible that some of the

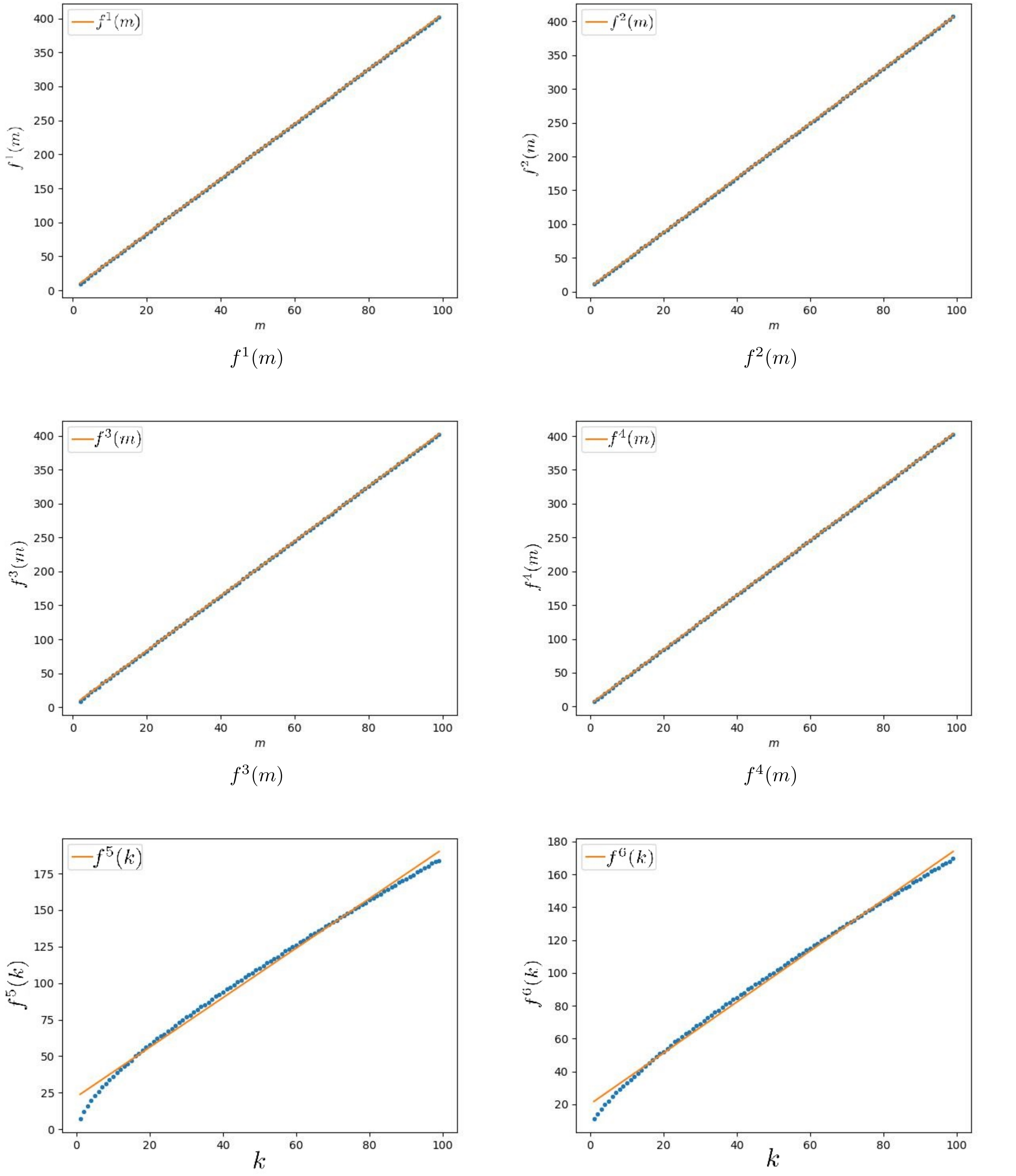

$f^1(m)$ $f^2(m)$

$f^3(m)$ $f^4(m)$

$f^5(k)$ $f^6(k)$

Fig. 10. The linear relationship between m (or parameter k for f^5 and f^6) and κ for curves $f_m^1, \cdots, f_k^6$ when ε = 0.01, where the blue points are specific experimental results and the yellow line is the image of the polynomial-fitted function.

TABLE III
THE m (OR PARAMETER k FOR f^7 AND f^8) AND κ FUNCTIONALS OF $f_k^7, \cdots, f_m^{15}$ FOR DIFFERENT ε CASES.

f_m^n (resp. f_k^n)	q	ε	$f^n(m)$ (resp. $f^n(k)$)
$f_k^7 = \frac{\kappa}{\Theta}$	1	0.01	$\kappa = 2.125k + 35.62$
		0.005	$\kappa = 2.592k + 51.23$
		0.001	$\kappa = 4.572k + 115.7$
	1.5	0.01	$\kappa = 1.845k + 26.3$
		0.005	$\kappa = 2.199k + 37.66$
		0.001	$\kappa = 3.689k + 85.31$
$f_k^8 = \frac{\kappa}{\Theta-1}$	1	0.01	$\kappa = 1.79k + 26.91$
		0.005	$\kappa = 2.121k + 38.22$
		0.001	$\kappa = 3.513k + 85.52$
	1.5	0.01	$\kappa = 1.646k + 21.82$
		0.005	$\kappa = 1.916k + 31.08$
		0.001	$\kappa = 3.05k + 69.82$
$f_m^9 = \frac{\kappa}{\Gamma-m}$	1	0.01	$\kappa = 2.125m + 35.62$
		0.005	$\kappa = 2.592m + 51.23$
		0.001	$\kappa = 4.572m + 115.7$
	1.5	0.01	$\kappa = 4.492m + 5.185$
		0.005	$\kappa = 6.106m + 7.891$
		0.001	$\kappa = 12.88m + 18.79$
$f_m^{10} = \frac{\kappa}{\Gamma-m-1}$	1	0.01	$\kappa = 1.79m + 26.91$
		0.005	$\kappa = 2.121m + 38.22$
		0.001	$\kappa = 3.513m + 85.52$
	1.5	0.01	$\kappa = 4.479m + 5.128$
		0.005	$\kappa = 6.088m + 7.361$
		0.001	$\kappa = 12.84m + 16.75$
$f_m^{11} = \frac{\kappa+\lfloor\frac{m}{2}\rfloor}{\Gamma-\lceil\frac{m}{2}\rceil}$	1	0.01	$\kappa = 7.557m + 6.167$
		0.005	$\kappa = 10.51m + 9.051$
		0.001	$\kappa = 22.92m + 21.68$
	1.5	0.01	$\kappa = 6.375m + 2.603$
		0.005	$\kappa = 8.914m + 4.073$
		0.001	$\kappa = 19.59m + 10.03$
$f_m^{12} = \frac{\kappa+\lfloor\frac{m}{2}\rfloor}{\Gamma-\lceil\frac{m}{2}\rceil-1}$	1	0.01	$\kappa = 7.538m + 5.219$
		0.005	$\kappa = 10.48m + 7.238$
		0.001	$\kappa = 22.86m + 16.11$
	1.5	0.01	$\kappa = 6.367m + 3.324$
		0.005	$\kappa = 8.905m + 4.715$
		0.001	$\kappa = 19.57m + 10.57$
$f_m^{13} = \frac{\kappa+m}{\Gamma-m}$	1	0.01	$\kappa = 2.605m + 51.1$
		0.005	$\kappa = 3.269m + 72.95$
		0.001	$\kappa = 6.083m + 164.3$
	1.5	0.01	$\kappa = 6.751m + 11.13$
		0.005	$\kappa = 9.292m + 15.97$
		0.001	$\kappa = 19.99m + 36.69$
$f_m^{14} = \frac{\kappa+m}{\Gamma-m-1}$	1	0.01	$\kappa = 2.121m + 38.22$
		0.005	$\kappa = 2.589m + 54.01$
		0.001	$\kappa = 6.007m + 86.49$
	1.5	0.01	$\kappa = 6.734m + 8.349$
		0.005	$\kappa = 9.267m + 11.81$
		0.001	$\kappa = 19.94m + 26.42$
$f_m^{15} = \frac{\kappa+2m}{\Gamma}$	1	0.01	$\kappa = 14.12m + 8.069$
		0.005	$\kappa = 20m + 12.11$
		0.001	$\kappa = 44.88m + 25.48$
	1.5	0.01	$\kappa = 11.51m + 6.214$
		0.005	$\kappa = 16.31m + 9.148$
		0.001	$\kappa = 36.54m + 21.02$

extreme points may not be presented in the figures. In this paper q is chosen to be 1 and 1.5, and when q = 1.5 (an integer plus $\frac{1}{2}$), the function curve is oscillating up and down. However, through Fig. 13-21, it can be found that when x is large, the image tends to be smooth, so it does not affect the selection of the knee point. Through Fig. 11 it can be found that the trend of $f^9(m)$ and $f^{10}(m)$, $f^{11}(m)$ and $f^{12}(m)$, and $f^{14}(m)$ and $f^{14}(m)$, is consistent in sampling points, which shows that adding or subtracting a constant to the denominator does not have a particularly large effect on the linear relationship between m and κ. However, the difference between sample points trends for $f^{11}(m)$, $f^{12}(m)$, $f^{15}(m)$ and $f^9(m)$, $f^{10}(m)$, $f^{13}(m)$, $f^{14}(m)$ show that when the coefficients in front of m are changed, the trend of the sampling points also changes significantly.

V. REMARK ON CONSTRAINED EMBEDDING OF ALL FRACTIONAL (g, f)-FACTORS

Lu [20] introduced all fractional factors and determined the necessary and sufficient condition for a graph which admits all fractional (g, f)-factors. Specifically, a graph G has all fractional (g, f)-factors if G has a fractional p-factor for each $p : V(G) \to \mathbb{R}^+$ satisfying $g(v) \leq p(v) \leq f(v)$ for any $v \in V(G)$. In data transmission networks, a network graph has all fractional (g, f)-factor implying the data packets within a given capacity range which can be transmitted at a certain moment.

Although the fractional factor, especially the all fractional factors, has been studied in rich literature, it seems that there is still a certain gap lying in specific network applications. The distinguishing facet of challenges in all fractional (g, f)-factors mainly focused on function embedding. When the analytical expressions of the two functions g and f are

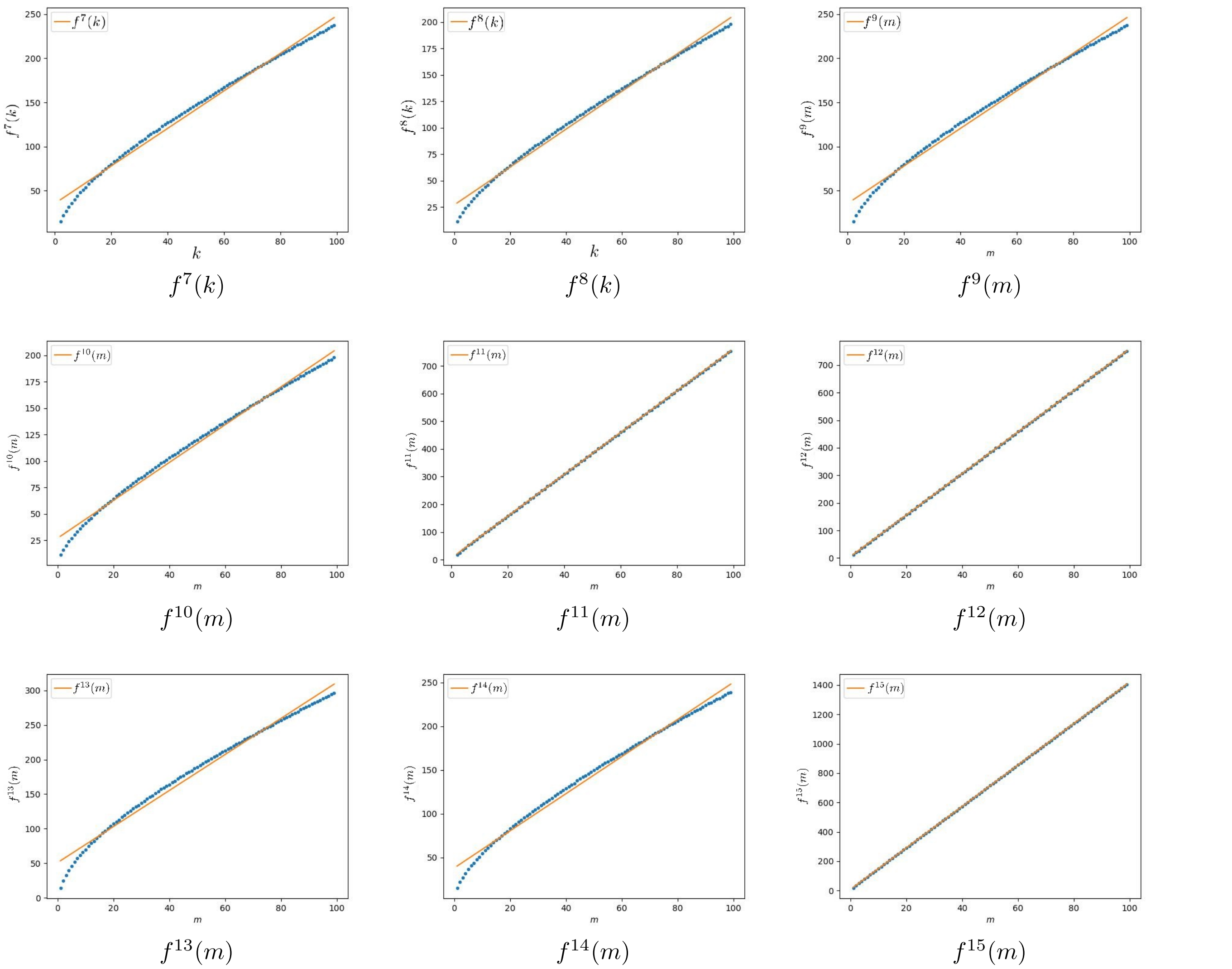

Fig. 11. The linear relationship between m (resp. k) and κ for curves $f_k^7, \cdots, f_m^{15}$ when $\varepsilon = 0.01$ and $q = 1$, where the blue points are specific experimental results and the yellow line is the image of the polynomial-fitted function.

determined in terms of the characteristics of the vertices (e.g., the capacity of uplink and downlink of channels associated with the site, the throughput of the site, the size of the site model, etc.) in the network graph, theoretically any function p between g and f is permissible. However, in specific applications, due to the similarity between associated vertices, there is a close correlation between the fractional degrees of adjacent vertices, which leads the function p satisfying a certain smoothness in continuous space, and oscillate arbitrarily is not allowed (the detailed interpretation will be presented in the next section).

Based on the aforementioned truths, this paper considers the embedding problem of function p in all fractional factor setting. Our contributions can be summarized as follows. With the aid of the dimensionality reduction operator, the high-dimensional graph data is reduced to 1-dimensional value, and thus the functions g, f, and p are visualized on the 2-D plane. Under this assumption, the criterion of function p embedding is given from a mathematical point of view.

The remainder of this paper is organized as follows. First, we make a rationale for the assumption of graph dimensionality reduction to ensure that the discussion of embeddings is meaningful. Secondly, the constraints of function p embedding are given and analyzed. Finally, some open problems on embedding are given.

A. Preliminary knowledge

The purpose of this section is to provide some basic concepts and assumptions, and make the necessary explanation.

1) Dimensionality reduction operator on graphs: Suppose that the network structure is modelled by a graph $G = (V(G), E(G))$, where the vertex set $V(G)$ expresses the set of sites and the edge set $E(G)$ denotes the set of channels in the network. Due to each site involving a lot of information in reality applications, we assume that each vertex in the network graph is expressed by a d-dimensional vector, then the g, f and p are functions denoted by $g, p, f : \mathbb{R}^d \to \mathbb{R}^+$. From this prospect, we have to discuss the function embedding problem in high-dimensional space. It can be simplified into a lower dimensional problem: assuming that there is a dimensionality reduction operator ϕ to map the multidimensional graph data to real numbers, i.e., $\phi : \mathbb{R}^d \to \mathbb{R}$. This operator maps the entire network graph from a high-dimensional space to a one-dimensional

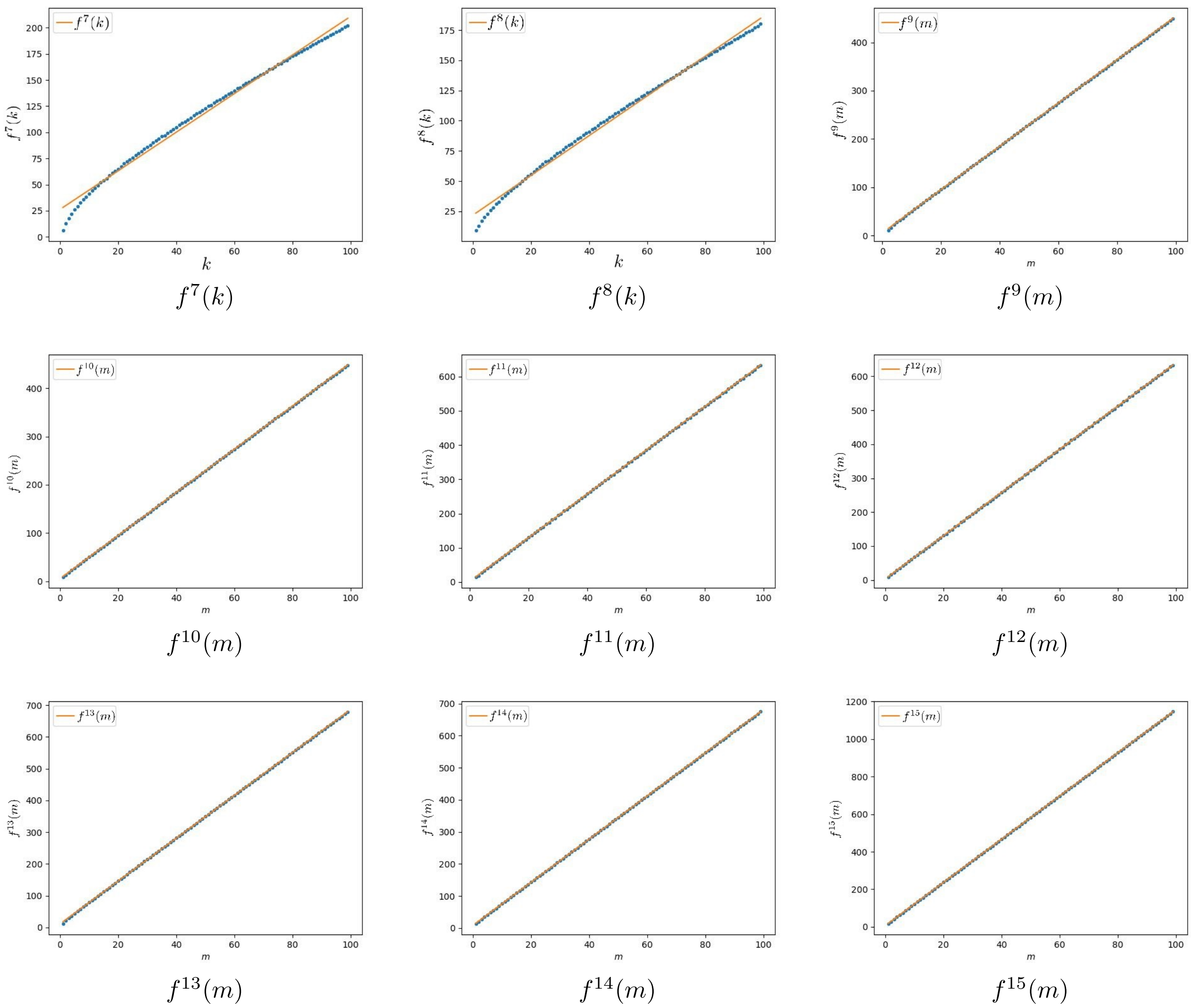

Fig. 12. The linear relationship between m (resp. k) and κ for curves $f_k^7(\kappa), \cdots, f_m^{15}(\kappa)$ when ε = 0.01 and $q = 1.5$, where the blue points are specific experimental results and the yellow line is the image of the polynomial-fitted function.

real number axis, and mapping each vertex to a real number. In this way, g, p, f can be regarded as a function from the real number axis to $\mathbb{R}^+$, and hence g, p, f can be visualization on the 2-D plane.

It is worth noting that dimensionality reduction operators on graphs are ubiquitous in data representations. For instance, in the ontology learning algorithm, the ontology topology structure is represented by a graph, each vertex represents a concept, edge represents the direct association between two concepts, and all the information related to the concept is encapsulated in a d-dimensional vector. The aim of ontology learning is to infer an optimal ontology function $\phi : V(G) \rightarrow \mathbb{R}$ in terms of ontology sample learning, that is, ϕ maps the entire ontology graph to the real number axis, and maps each vertex to a real number. Such ontology function is actually a class of dimensionality reduction operator, which can be formalized by $\phi : \mathbb{R}^d \rightarrow \mathbb{R}$. Another crucial fact lies in that adjacent vertices are often mapped to close points on the real axis, since these vertices have high similarities with each other.

2) Continuous and smoothness: To derive the main idea of this remark, we attempt to make further restrictions and specifications on the mathematical framework. First, we propose $V \subset \mathbb{R}$ to be limited in a certain range which serves as a continuized space into which all vertices are mapped. In this way, both g and f can be considered as continuous functions on V where $g(v)$ and $f(v)$ for all vertices are mapped. Hence, p is also regarded as a continuous function on V satisfying $g \leq p \leq f$.

Second, the extant graph data reveal that for vertex functions, the distribution of its values has dramatical rules to follow. Specifically, adjacent vertices on the graph always share close function values, so that the vertex function manifests a smooth continuous distribution state without violent jitter. Intuitively, this feature fits the characteristics of data transmission networks. For network data transmission, large data packets are transmitted through multiple channels after cutting. The more adjacent vertices require the capacity and computing ability of the corresponding sites to be similar, and only in this way can sites meet the requirements of smooth data transmission. It's just like this: cities near megacities are often economically developed areas, and there will be no large areas of deserts or mountains. Based on this observation, in what follows, we assume that both the g and f

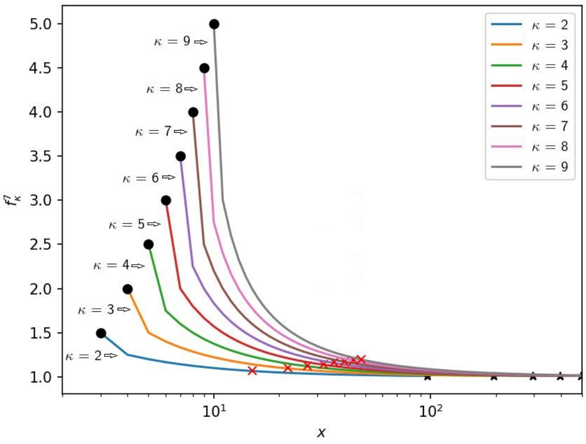

ε = 0.01 and $q = 1$

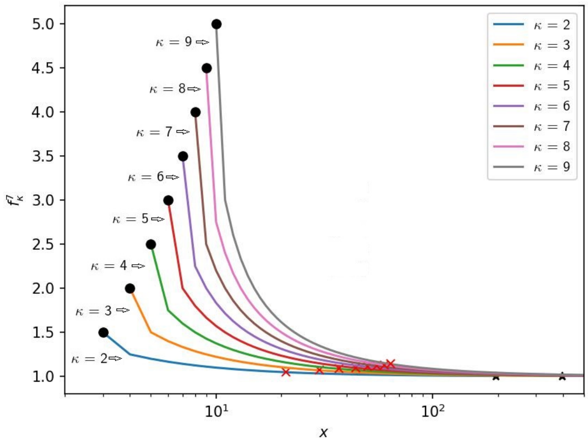

ε = 0.005 and $q = 1$

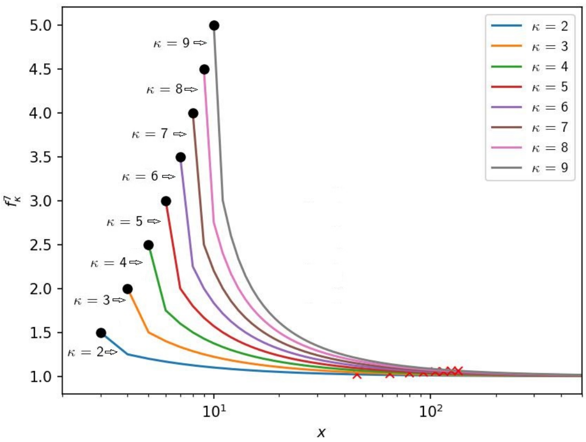

ε = 0.001 and $q = 1$

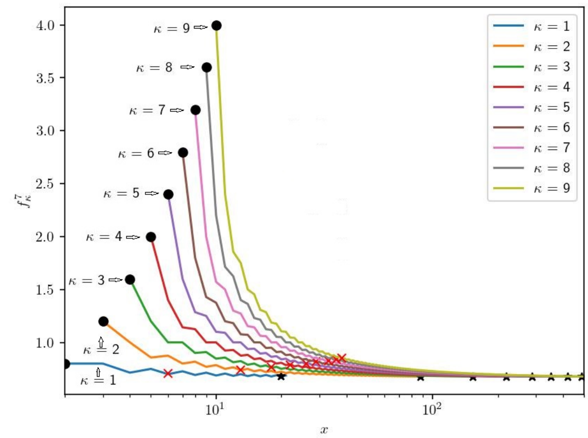

ε = 0.01 and $q = 1.5$

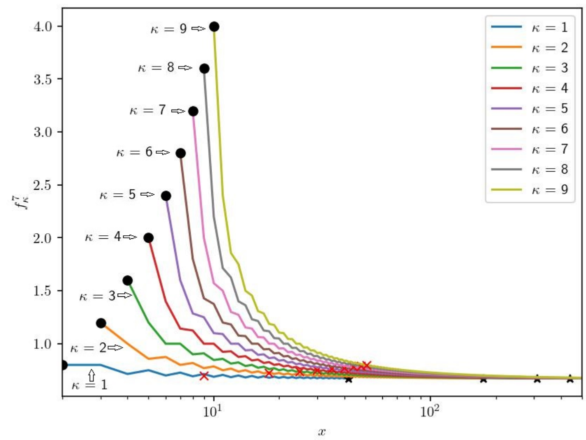

ε = 0.005 and $q = 1.5$

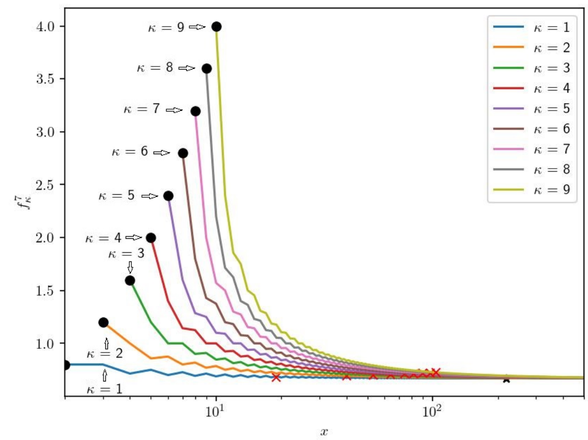

ε = 0.001 and $q = 1.5$

Fig. 13. The curve f_k^7 of $k \in [1, 9]$, where the black dots and pentagrams represent the extreme points, and the red $\times$ represents the global knee point of the function.

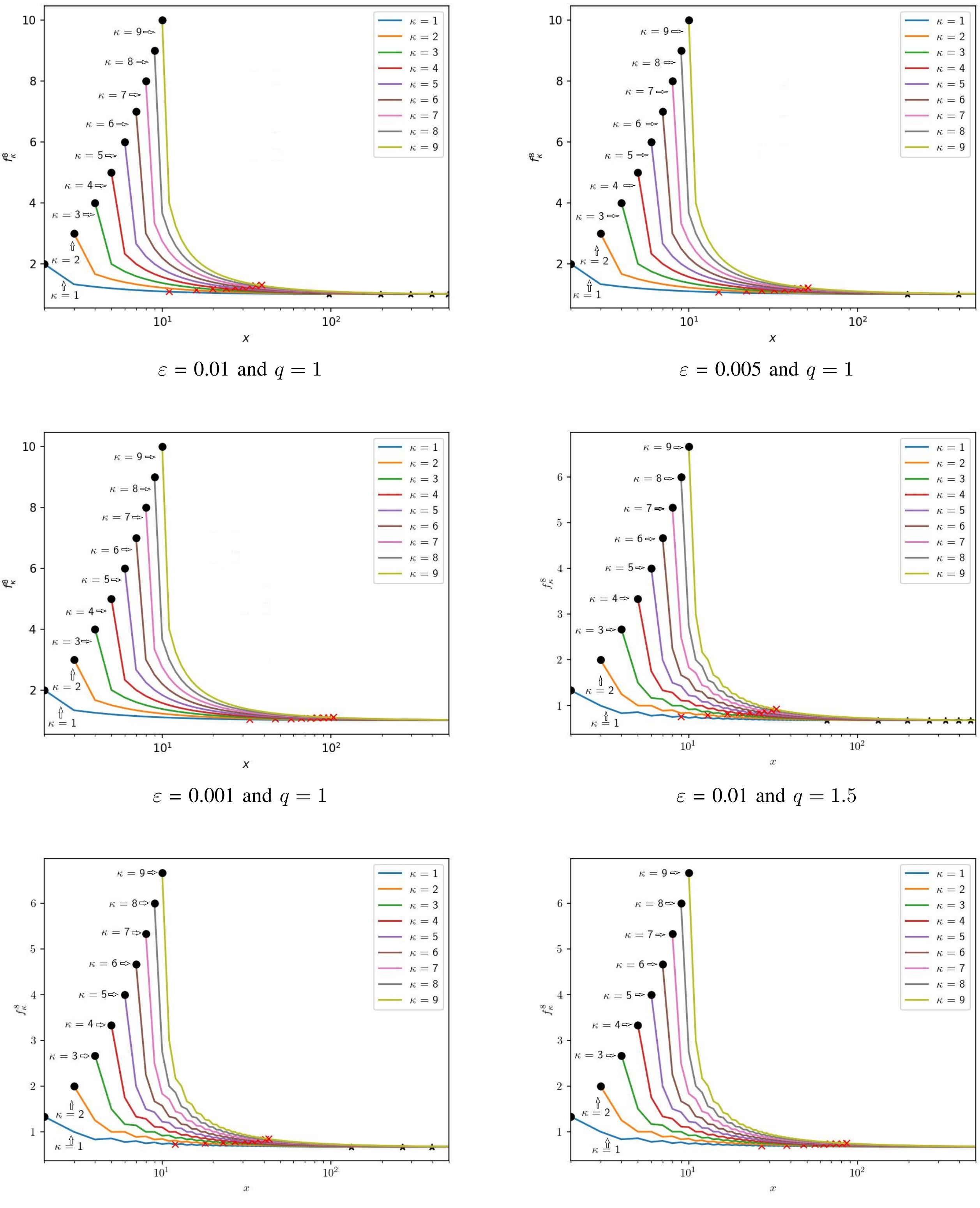

ε = 0.01 and $q = 1$

ε = 0.005 and $q = 1$

ε = 0.001 and $q = 1$

ε = 0.01 and $q = 1.5$

ε = 0.005 and $q = 1.5$

ε = 0.001 and $q = 1.5$

Fig. 14. The curve f_k^8 of $k \in [1, 9]$, where the black dots and pentagrams represent the extreme points, and the red $\times$ represents the global knee point of the function.

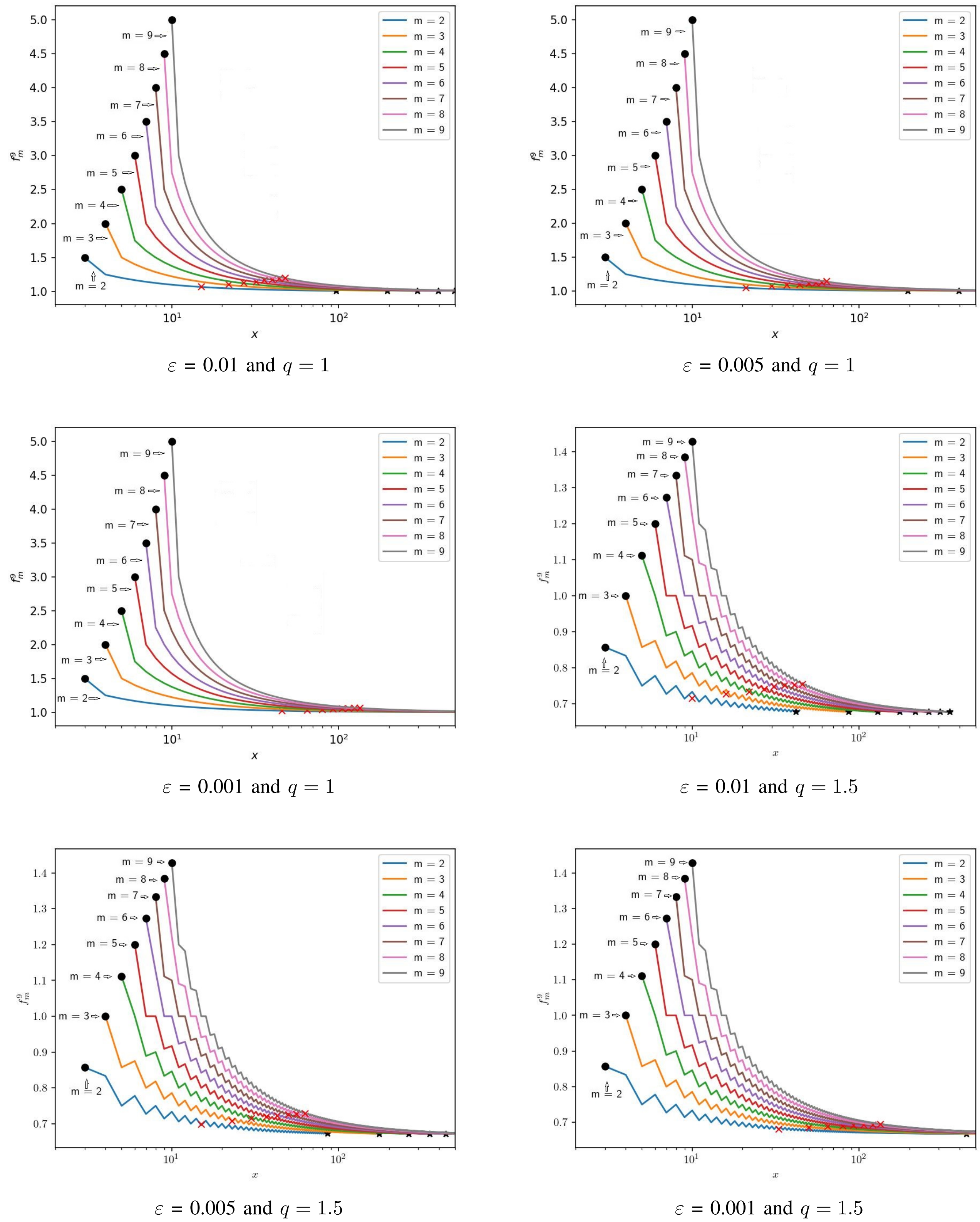

Fig. 15. The curve f_m^9 of $m \in [1, 9]$, where the black dots and pentagrams represent the extreme points, and the red $\times$ represents the global knee point of the function.

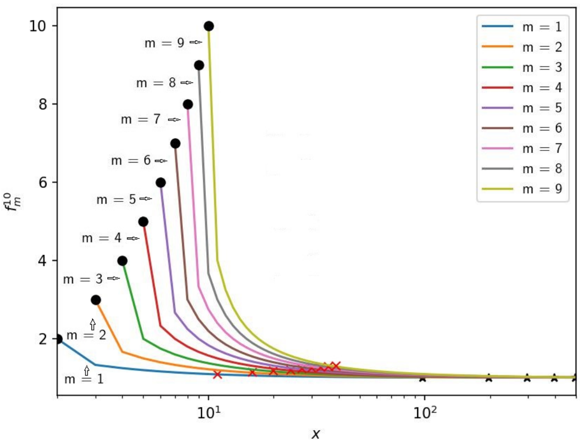

ε = 0.01 and $q = 1$

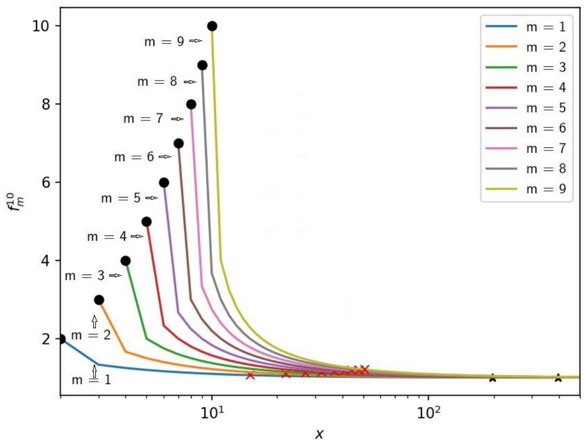

ε = 0.005 and $q = 1$

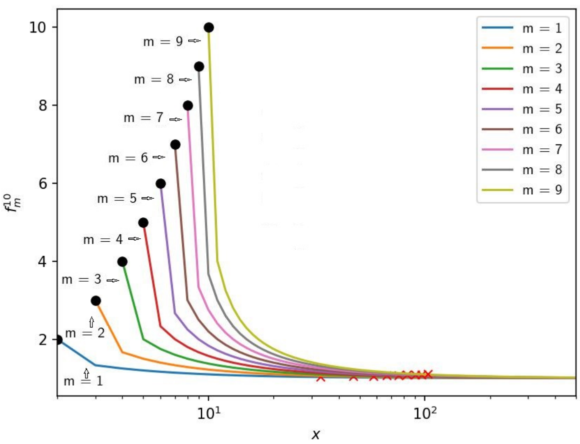

ε = 0.001 and $q = 1$

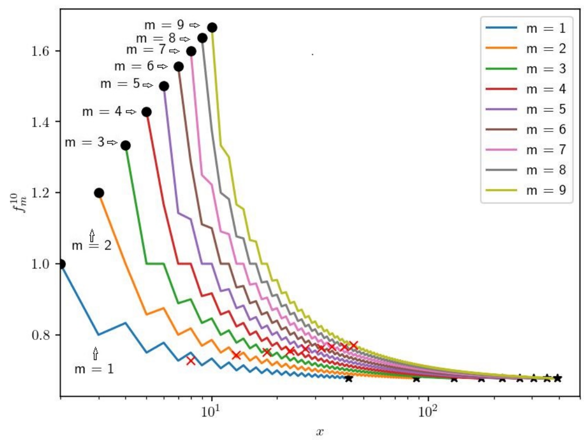

ε = 0.01 and $q = 1.5$

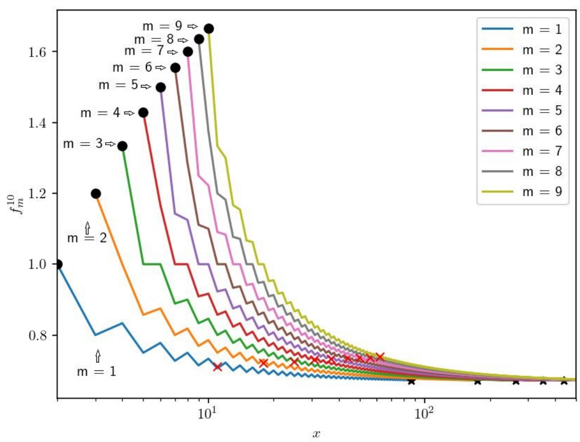

ε = 0.005 and $q = 1.5$

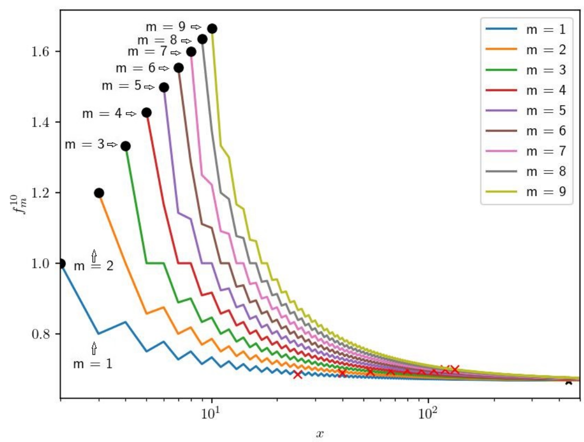

ε = 0.001 and $q = 1.5$

Fig. 16. The curve f_m^{10} of $m \in [1, 9]$, where the black dots and pentagrams represent the extreme points, and the red $\times$ represents the global knee point of the function.

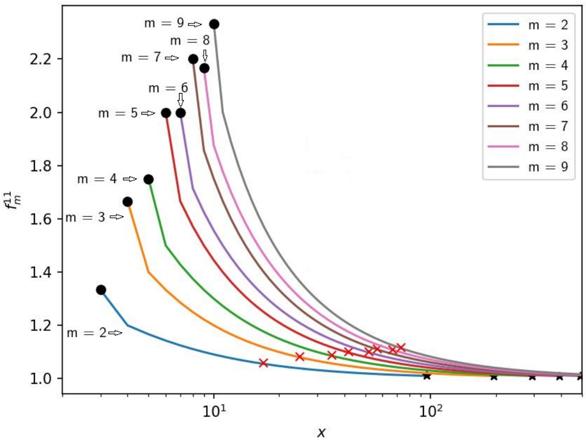

ε = 0.01 and $q = 1$

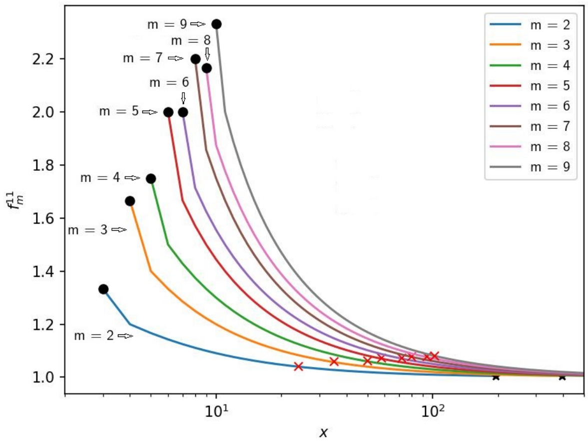

ε = 0.005 and $q = 1$

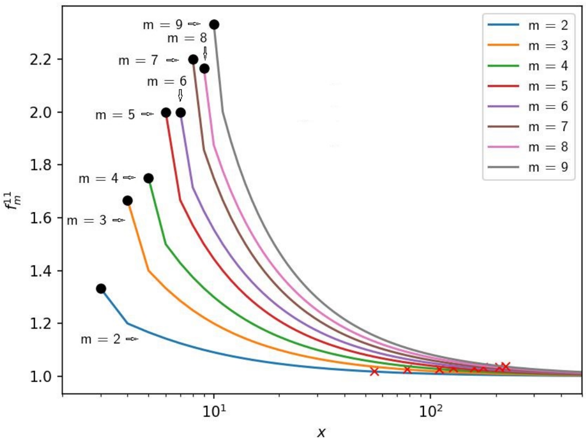

ε = 0.001 and $q = 1$

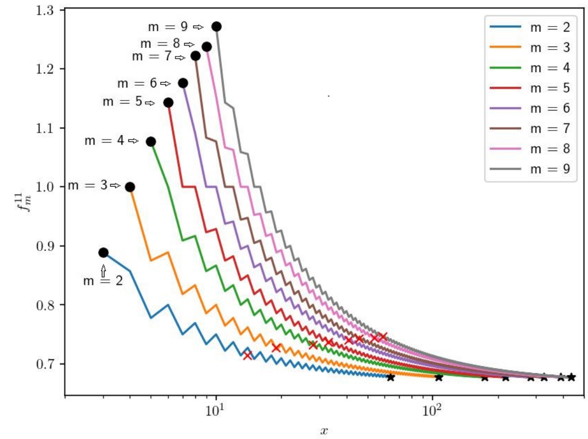

ε = 0.01 and $q = 1.5$

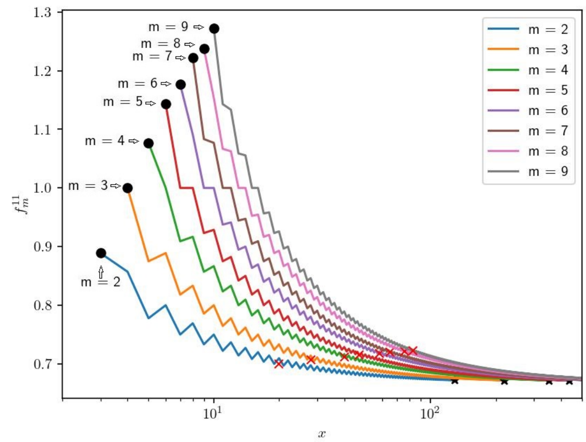

ε = 0.005 and $q = 1.5$

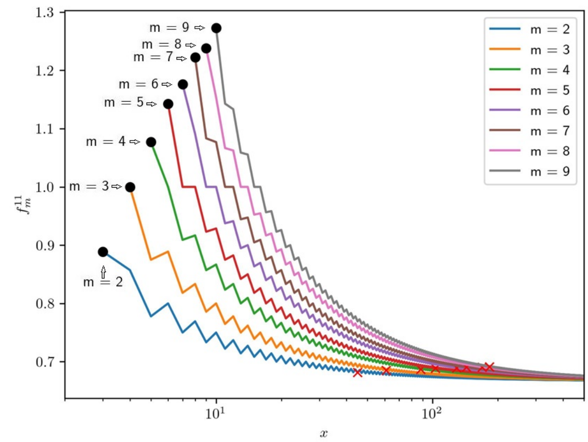

ε = 0.001 and $q = 1.5$

Fig. 17. The curve f_m^{11} of $m \in [1, 9]$, where the black dots and pentagrams represent the extreme points, and the red $\times$ represents the global knee point of the function.

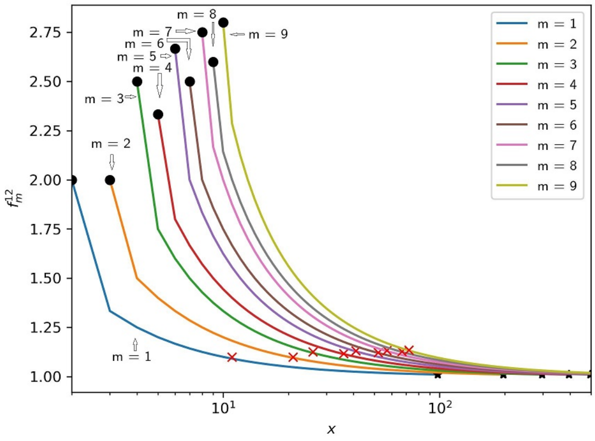

ε = 0.01 and $q = 1$

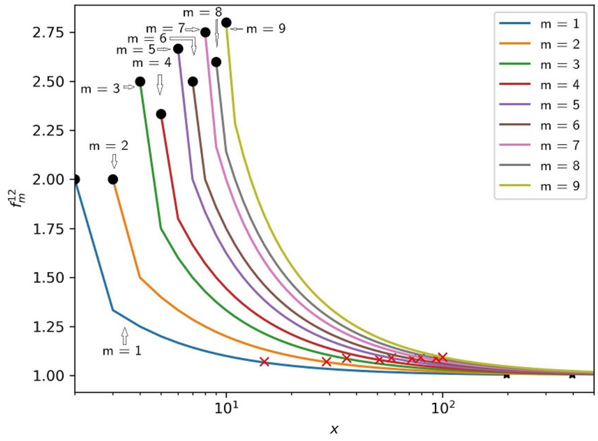

ε = 0.005 and $q = 1$

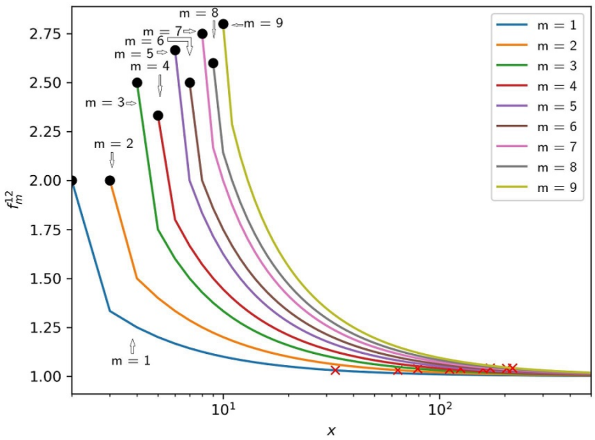

ε = 0.001 and $q = 1$

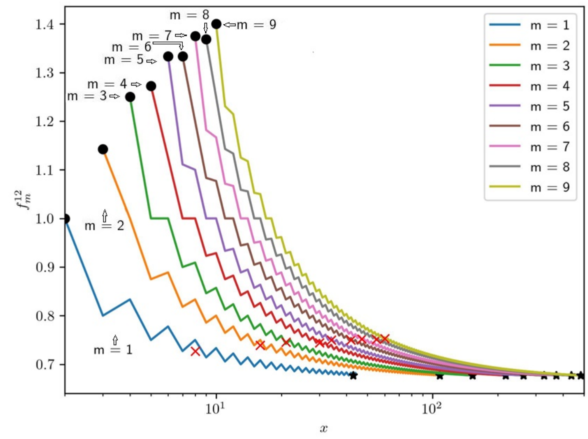

ε = 0.01 and $q = 1.5$

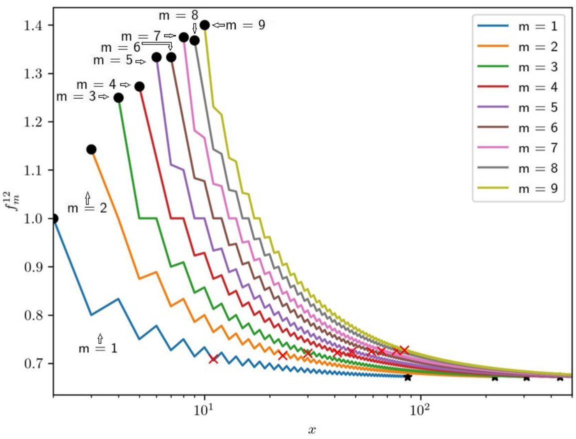

ε = 0.005 and $q = 1.5$

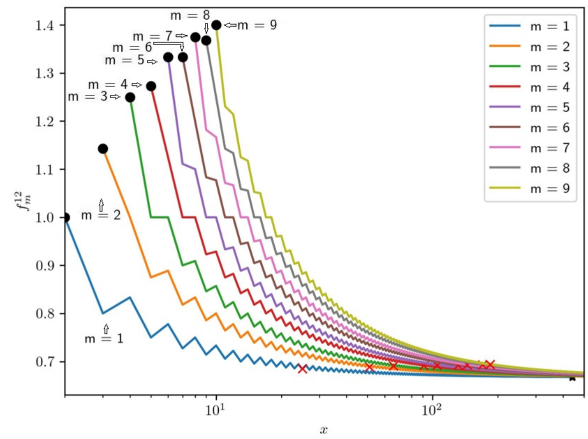

ε = 0.001 and $q = 1.5$

Fig. 18. The curve f_m^{12} of $m \in [1, 9]$, where the black dots and pentagrams represent the extreme points, and the red $\times$ represents the global knee point of the function.

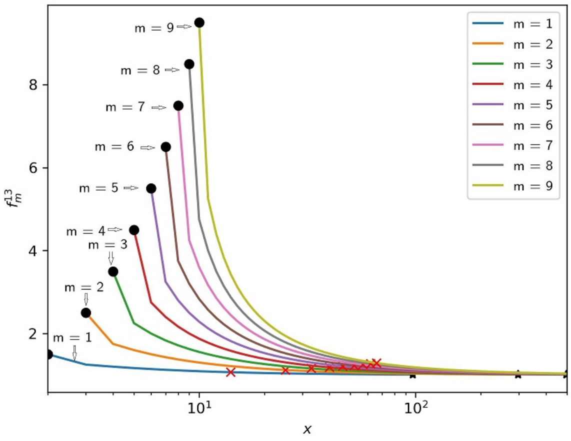

ε = 0.01 and $q = 1$

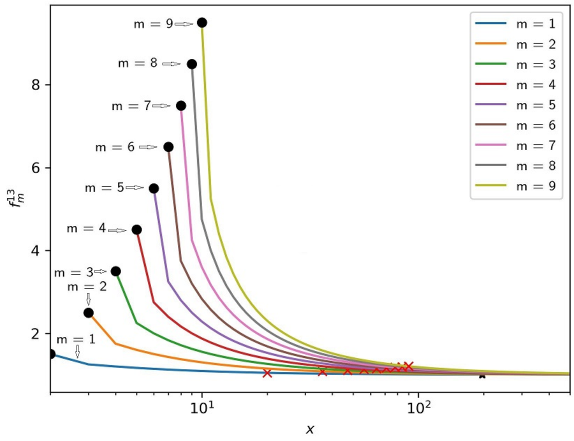

ε = 0.005 and $q = 1$

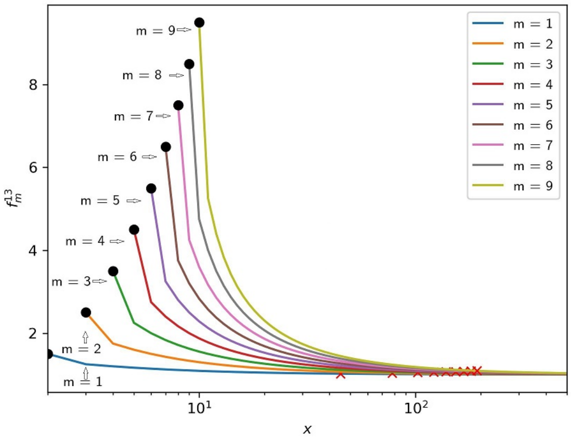

ε = 0.001 and $q = 1$

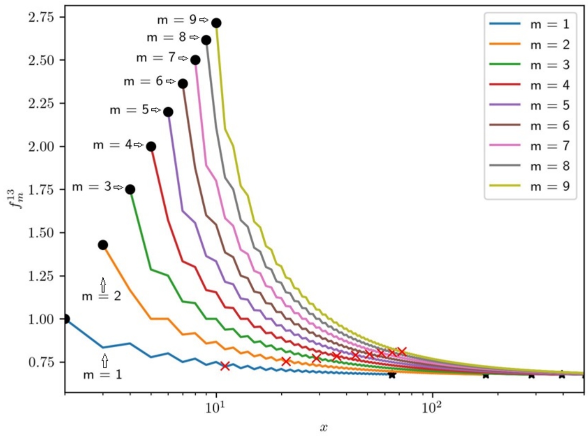

ε = 0.01 and $q = 1.5$

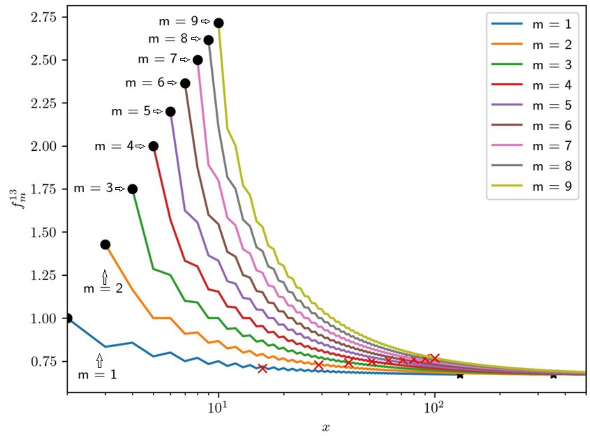

ε = 0.005 and $q = 1.5$

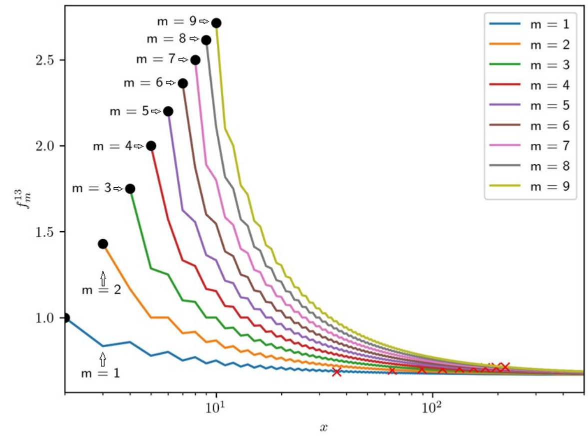

ε = 0.001 and $q = 1.5$

Fig. 19. The curve f_m^{13} of $m \in [1, 9]$, where the black dots and pentagrams represent the extreme points, and the red $\times$ represents the global knee point of the function.

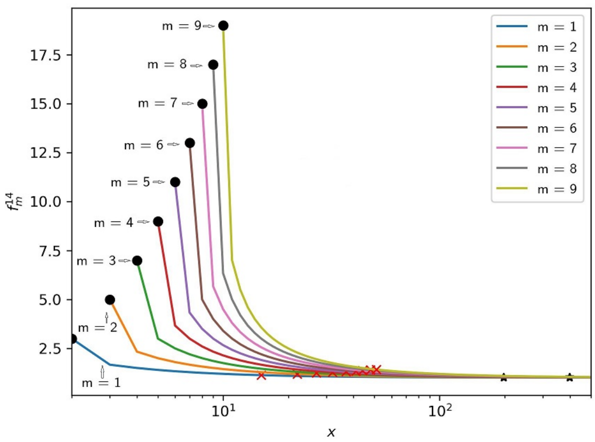

ε = 0.01 and $q = 1$

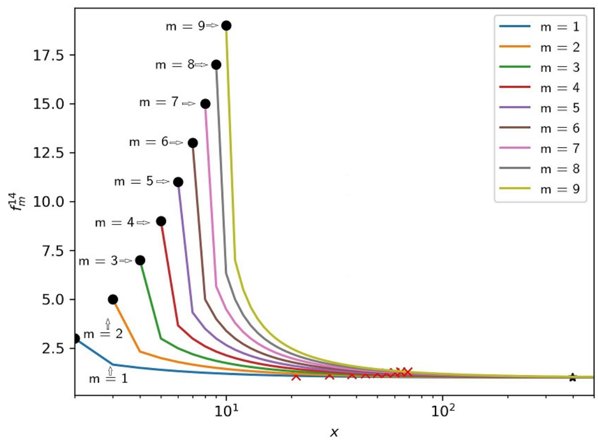

ε = 0.005 and $q = 1$

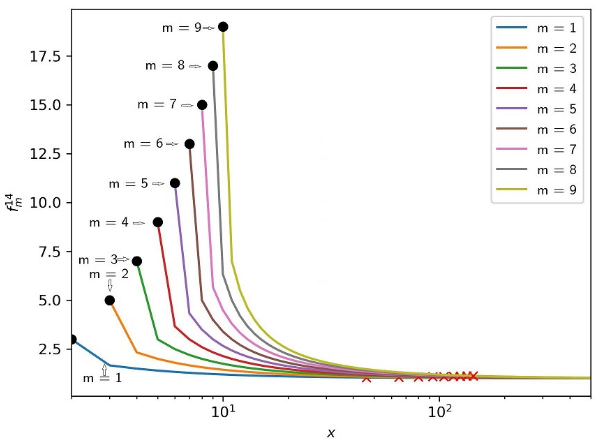

ε = 0.001 and $q = 1$

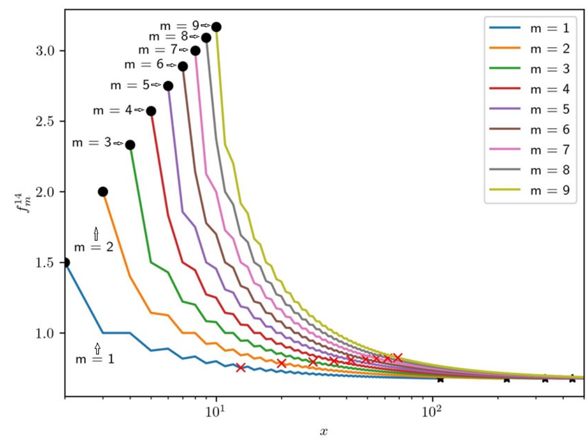

ε = 0.01 and $q = 1.5$

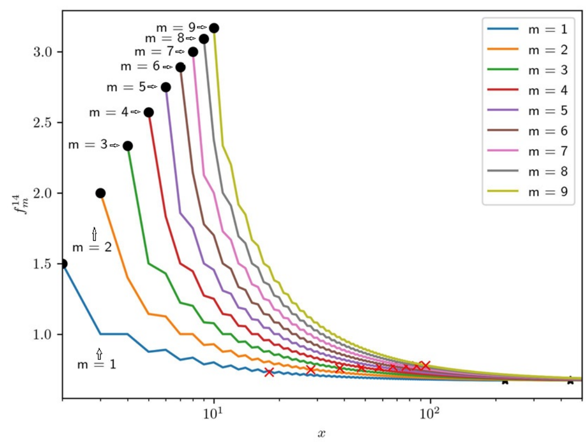

ε = 0.005 and $q = 1.5$

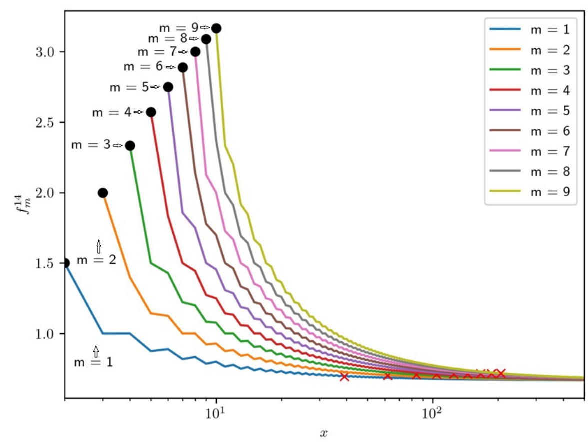

ε = 0.001 and $q = 1.5$

Fig. 20. The curve f_m^{14} of $m \in [1, 9]$, where the black dots and pentagrams represent the extreme points, and the red $\times$ represents the global knee point of the function.

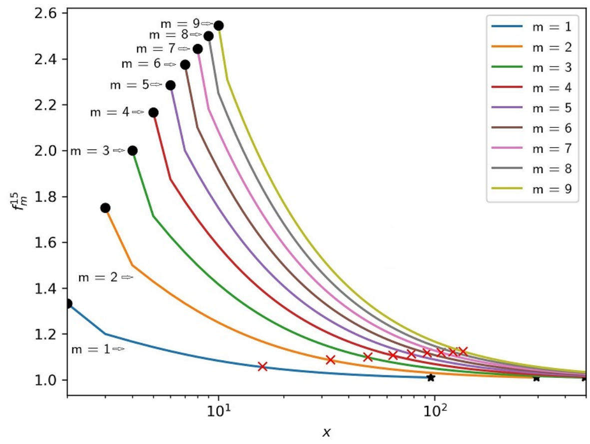

ε = 0.01 and $q = 1$

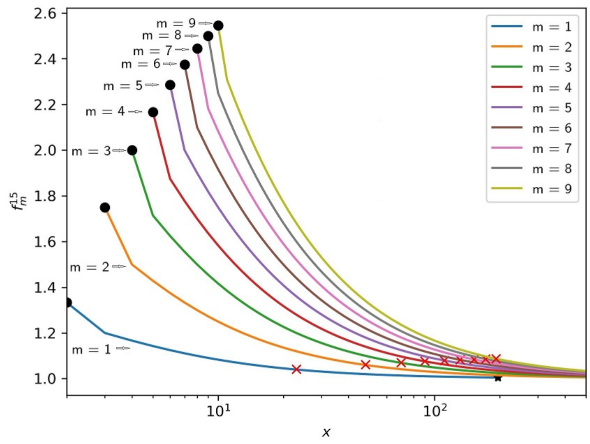

ε = 0.005 and $q = 1$

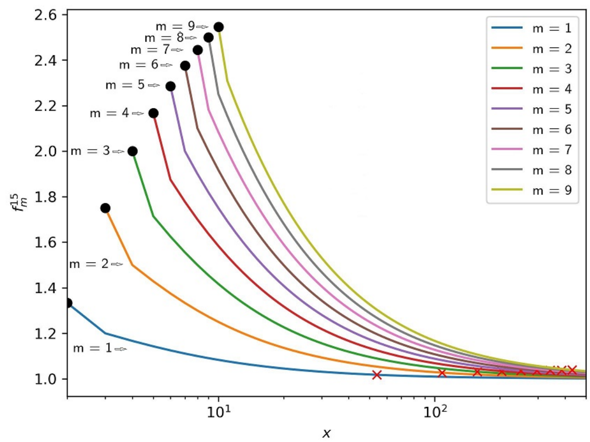

ε = 0.001 and $q = 1$

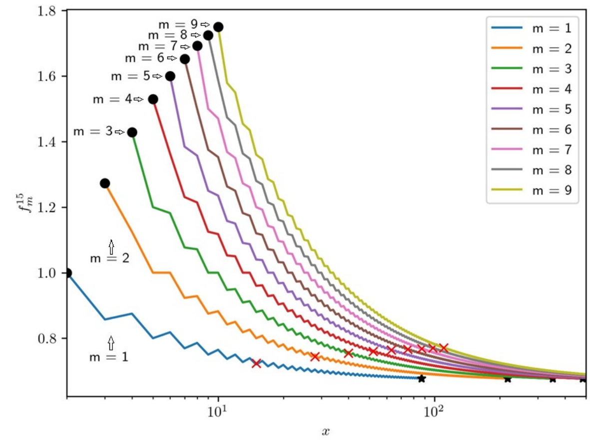

ε = 0.01 and $q = 1.5$

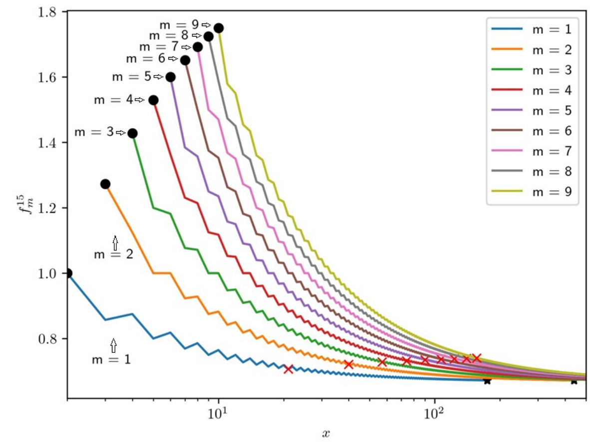

ε = 0.005 and $q = 1.5$

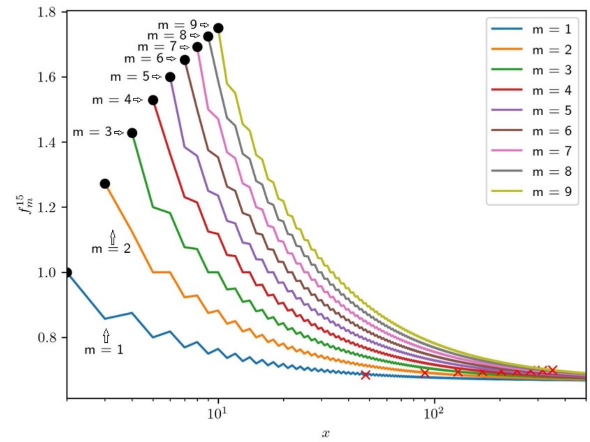

ε = 0.001 and $q = 1.5$

Fig. 21. The curve f_m^{15} of $m \in [1, 9]$, where the black dots and pentagrams represent the extreme points, and the red $\times$ represents the global knee point of the function.

are smooth functions that do not experience violent jittering.

Since g and f are upper bound and lower bound functions of vertex fractional degree, we can further assume that they are "shape consistency". Specifically, the following two conditions are satisfied:
(1) g and f obey the same type of distribution.
(2) The peaks (or symmetry axes, or inflection points) of g and f are close.

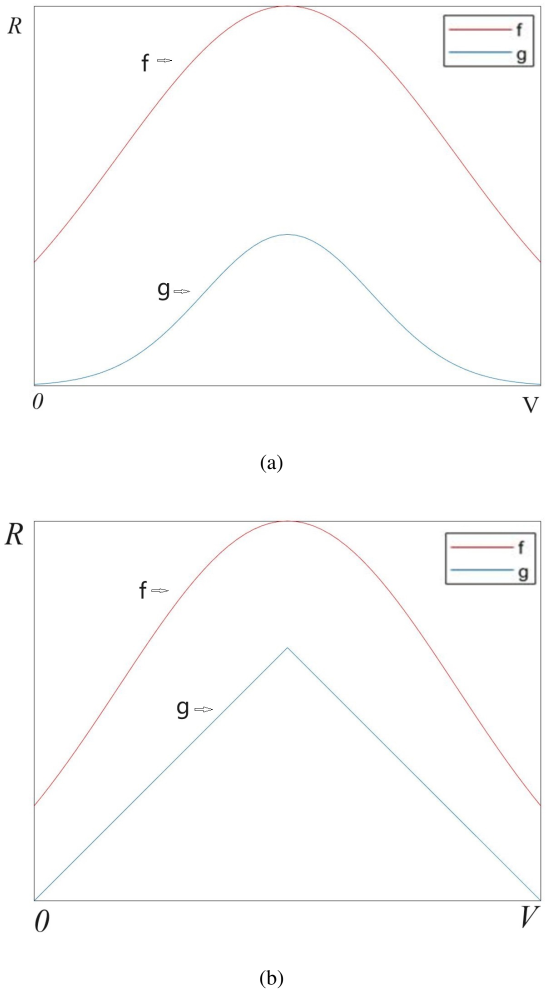

Fig. 22. Functions g and f with shape consistency (Figure 22(a)) and different types of distribution (Figure 22(b)).

Both g and f in Figure 22(a) belong to Gaussian distribution and this case belongs to shape consistency. In Figure 22(b), g and f do not obey the same type of distribution; in Figure 23, although g and f share the same type of distribution, their symmetry axes are far apart, so in this case g and f do not satisfy shape consistency.

B. Formal statement of embedding problem

When the expressions of functions g and f are determined, theoretically speaking, any form of p between g and f is allowable. However, for practical applications, most of the functions p have no real physical meaning, and they only exist in mathematical possibilities. Imagining that the function p randomly walks between g and f, although it is allowed from the definition of the all fractional (g, f)-factors,

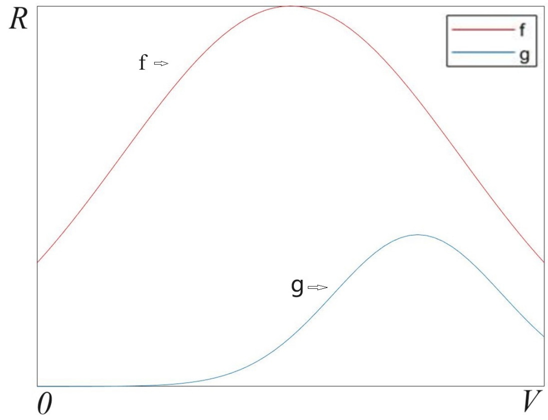

Fig. 23. Functions g and f with large gap of symmetry axes.

such a function p is meaningless for a data transmission network. As observed and discussed before, the function p should also present a certain regularity like functions g and f, which reflect the dynamic change of fractional degree between vertices (e.g., the value of p of adjacent vertices changes smoothly).

Since function p is constrained by $g \leq p \leq f$, we call p as an *embedding* of all fraction (g, f)-factors. If p fits the requirements of specific practical applications and exhibits certain good characteristics, we say p is a good embedding, and otherwise p has no meaningful interpretation is called a bad embedding. The main purpose of this remark is to discuss the embedding problem in all fractional factor setting. There are several thought-provoking questions: (1) What kind of embedding is a good embedding? (2) How to formally define embedding from a mathematical prospect?

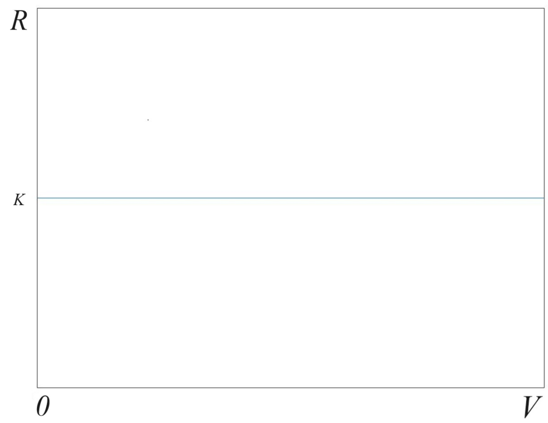

Fig. 24. There is no embedding problem for fractional k-factor.

We first discuss these issues from intuition. Clearly, the embedding problem does not exist if $g(v) = f(v) = k$ for any $v \in V(G)$ in all fractional (g, f)-factors setting (refer to Figure 24). In all fractional $[a, b]$-factors setting, all embedded p functions are bounded in a band area in the 2D plane which is formed by the parallel curves of g and f. Figure 25(a) shows two embeddings p_1 (good embedding) and p_2 (seems bad). To be more general, two embeddings p_1 (good embedding) and p_2 (seems bad) are embedded into

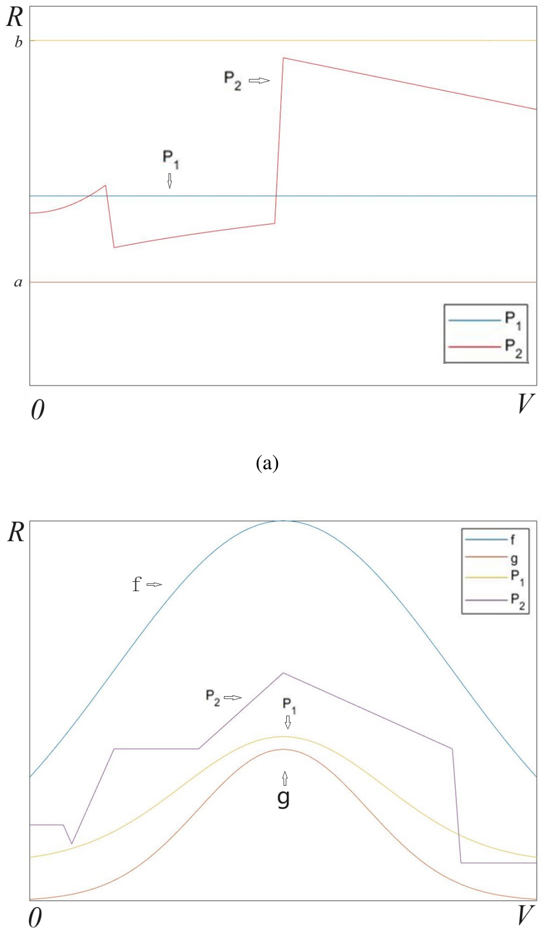

(a)

(b)

Fig. 25. Embeddings p_1 and p_2 in all fractional $[a, b]$-factors.

2-D area formed by lower and upper functions g and f in general all fractional (g, f)-factors setting (see Figure 25(b)). Intuitively, under the assumption that function g and f are smooth and have similar shapes and axes of symmetry, if the surface shape of function h is similar to that of the g and f, and there are also approximate values of peaks and valleys, then it can be considered a good embedding. If function p is oddly shaped, or the curve oscillates wildly, it is considered as a bad embedding.

Therefore, this remark considers key questions about the embedding of function h: what reasonable restrictions should be forced on the embedding, and how to characterize it mathematically in a formal way? We answer these questions in the next section, and our inspiration comes from embedding problems in 2-type fuzzy set.

C. Constrained embedding

A naive way to get the good embedding is to shift the curve of function f down, or move up the curve of function g function, and thus to get the embedding function h. The advantage of this approach lies in the function h maintains the characteristics of the g and f, which can well reflect the characteristics of the graph topological structure. The shortcoming is obvious, i.e., a lot of meaningful embeddings are lost. Now, we propose some constraints on embedding functions from a functional perspective:
(1) h is convex.
(2) h is l-Lipschitz, i.e., $|h(v) - h(v')| \leq l|v - v'|$ for any $v, v' \in V(G)$.

Suppose that f, g and h are defined in the high dimensional space where the representation of vertex v is also in the high-dimensional space. Then the above condition (2) can be formulated by
(2) h is l-Lipschitz, i.e., $\|h(v) - h(v')\| \leq l\|v - v'\|$ for any $v, v' \in V(G)$.
In addition, we further give the following constraint in high dimensional settings:
(3) h is α-smooth, i.e., $\| \bigtriangledown h(v) - \bigtriangledown h(v')\| \leq \alpha\|v - v'\|$ for any $v, v' \in V(G)$.

We say that an embedding h is a *well-defined embedding* if it satisfies conditions (1) and (2), and an embedding h (in high dimensional setting) is an *outstanding-defined embedding* if it satisfies conditions (1), (2) and (3). Note that these two newly defined concepts have specific meanings in practical applications, and the function h conforms to the general law of adjacent vertices changing in graphs. Accordingly, we introduce the following concepts as the constrained all fractional (g, f)-factors.

Definition 1: A graph G has well-defined all fractional (g, f)-factors if G has a fractional p-factor for each well-defined embedding $p : V(G) \rightarrow \mathbb{R}^+$ satisfying $g(x) \leq p(x) \leq f(x)$ for any $x \in V(G)$.

Definition 2: A graph G has outstanding-defined all fractional (g, f)-factors if G has a fractional p-factor for each outstanding-defined embedding $p : V(G) \rightarrow \mathbb{R}^+$ satisfying $g(x) \leq p(x) \leq f(x)$ for any $x \in V(G)$.
However, we currently do not know about the nature of the above two new concepts, which awaits our further study.

D. Conclusion and discussion

In this section, we formally introduce the embedding problem in all fractional (g, f)-factors setting, and discuss what is the good embedding we want in the reality applications. We raise the following open questions for future studies.

Problem 1: Are there sufficient and necessary conditions for the existence of well-defined all fractional (g, f)-factors (even in a very specific constrained setting)?

Problem 2: Are there sufficient and necessary conditions for the existence of outstanding-defined all fractional (g, f)-factors (even in a very specific constrained setting)?

VI. A COUNTEREXAMPLE OF $t(G)$ FOR FRACTIONAL $[a, b]$-FACTORS

Gao et al. [21] determined the sharp toughness bound for a graph admits a fractional $[a, b]$-factor, which is stated as follows.

Theorem 1: (Gao et al. [21]) Let a, b be integers with $2 \leq a \leq b$, and G be a graph. If G is a complete graph, then $|V(G)| \geq a + 1$. Then, G admits a fractional $[a, b]$-factor if $t(G) \geq a - 1 + \frac{a-1}{b}$.
In order to explain the sharpness of toughness bound in Theorem 1, the authors showcased the following counterexample (suppose $m \in \mathbb{N}$ and $2 \leq a \leq b$): $V(G) = A \cup B \cup C$ with $|A| = |B| = (mb+1)(a-1)$ and $|C| = m(a-1)$. Both A and C are cliques in G, and B is isomorphic to $(mb + 1)K_{a-1}$.

Other edges in G conclude a perfect matching between A and B, and the edges connect each pair of vertices between B and C.

To calculate the toughness of G, let $S = (A - \{x\}) \cup C$ where $x \in A$ if $a = 2$, and $S = (A - \{x\}) \cup \{y\} \cup C$ where $x \in A$ and $y \in B$ is a pair of matching in G if $a \geq 3$. Then

$$t(G) = \frac{|S|}{\omega(G_n - S)} = \begin{cases} \frac{mb+m}{mb+1}, & \text{if } a = 2 \\ \frac{(mb+m+1)(a-1)}{mb+2}, & \text{if } a \geq 3 \end{cases}$$

Clearly, we have $\lim_{m\to\infty} t(G) = a - 1 + \frac{a-1}{b}$.

It can be seen that if we select $S = C$ and $T = B$, then

$$b|S| - a|T| + d_{G-S}(T) = mb(a-1) - (mb+1)(a-1) < 0,$$

which implies G has no fractional $[a, b]$-factor by the sufficient and necessary condition of fractional $[a, b]$-factor.

Now, we present another counterexample to explain the sharpness of toughness bound in Theorem 1. Suppose $m \in \mathbb{N}$ and $2 \leq a \leq b$. $V(G) = A \cup B \cup C$ with $|A| = |B| = (mb-1)(a-1)$ and $|C| = m(a-1) - 1$. Both A and C are cliques in G, and B is isomorphic to $(mb-1)K_{a-1}$. Other edges in G conclude a perfect matching between A and B, and the edges connect each pair of vertices between B and C.

To calculate the toughness of G, let $S = (A - \{x\}) \cup C$ where $x \in A$ if $a = 2$, and $S = (A - \{x\}) \cup \{y\} \cup C$ where $x \in A$ and $y \in B$ is a pair of matching in G if $a \geq 3$. Then

$$t(G) = \frac{|S|}{\omega(G - S)} = \begin{cases} \frac{mb+m-3}{mb-1}, & \text{if } a = 2 \\ \frac{(mb+m-1)(a-1)-1}{mb}, & \text{if } a \geq 3 \end{cases}$$

Obviously, we get $\lim_{m\to\infty} t(G) = a - 1 + \frac{a-1}{b}$.

It can be seen that if we select $S = C$ and $T = B$, then

$$b|S| - a|T| + d_{G-S}(T) = mb(a-1) - b - (mb-1)(a-1) < 0,$$

which implies G has no fractional $[a, b]$-factor by the sufficient and necessary condition of fractional $[a, b]$-factor.

VII. Conclusion

In this paper, we address KPI problem of connectivity and toughness-related parameters for the existence of $\mathcal{H}$-factor in the case where one of the objective values is infinite, alleviate the decision maker's selection pressure for network construction by finding a family of knee points on curves varying with respect to m (resp. k), and then determining the dynamics of the relationship between κ and m (resp. k) under certain conditions through the knee points. Since these toughness-related variables characterize the needs of the network from different application perspectives, the knee point calculation approach given in this article facilitates network designers directly to obtain relevant network construction indicators.

The following issues can be considered as the future works:

- It is imperative to further infer the relationship between κ and m (resp. k) under different ε situations and generalize it to more realistic problems.
- Since $\mathcal{H}$-factor is a special family of fractional factors, the surfaces and balanced parameters for fractional factors in various settings are meaningful to be deeply studied, and the knee points of these settings also need to be calculated.

References

[1] W. Gao, Y. Chen, Y. Zhang, "Viewing the network parameters and $\mathcal{H}$-factors from the perspective of geometry," *International Journal of Intelligent Systems*, vol. 37, no. 10 pp. 6686–6728, 2022.

[2] V. Chvátal, "Tough graphs and Hamiltonian circuits," *Discrete Mathematics*, vol. 5, pp. 215–225, 1973.

[3] H. Enomoto, B. Jackson, P. Katerinis, A. Saito, "Toughness and the existence of k-factors," *Journal of Graph Theory*, vol. 9, pp. 87–95, 1985.

[4] J. Yang, Y. Ma, G. Liu, "Fractional (g, f)-factors in graphs," *Appl. Math. J. Chinese Univ. Ser. A*, vol. 16, pp. 385–390, 2001.

[5] Y. Ma, G. Liu, "Isolated toughness and the existence of fractional factors," *Acta Mathematica Scientia*, vol. 26, no. 1 pp. 133–140, 2003.

[6] S. Zhou, Z. Sun, H. Liu, "Sun touthness and $P_{\geq 3}$-factors in graphs," *Contributions to Discrete Mathematics*, vol. 14, no. 1 pp. 167–174, 2019.

[7] L. Zhu, H. M. Baskonus, W. Gao, "A variant of sun toughness and the existence of path factors in networks," Proceeding of ML4CS 2020, 3rd International Conference on Machine Learning for Cyber Security, Guangzhou China, Springer Publisher.

[8] D. Woodall, "The binding number of a graph and its Anderson number," *Journal of Combinatorial Theory, Series B*, vol. 15, pp. 225–225, 1973.

[9] W. Gao, Y. Chen, Y. Wang, "Network vulnerability parameter and results on two surfaces," *International Journal of Intelligent Systems*, vol. 36, no. 8 pp. 4392–4414, 2021.

[10] W. Wei, J. Shen, A. Telikani, M. Fahmideh, W. Gao, "Feasibility analysis of data transmission in partially damaged IoT networks of vehicles," *IEEE Transactions on Intelligent Transportation Systems*, vol. 24, no. 4 pp. 4577–4588, 2023.

[11] K. Li, H. Nie, H. Gao, X. Yao, "Posterior decision making based on decomposition-driven knee point identification," *IEEE Transactions on Evolutionary Computation*, vol. 26, no. 6 pp. 1409–1423, 2022.

[12] R. C. Purshouse, K. Deb, M. M. Mansor, S. Mostaghim, R. Wang, "A review of hybrid evolutionary multiple criteria decision making methods," in *IEEE Congress on evolutionary computation (CEC)*, pp. 1147–1154, 2014.

[13] G. Lai, M. Liao, K. Li, "Empirical studies on the role of the decision maker in interactive evolutionary multi-objective optimization," in *IEEE Congress on Evolutionary Computation (CEC)*, pp. 185–192, 2021.

[14] K. S. Bhattacharjee, H. K. Singh, M. Ryan, T. Ray, "Bridging the gap: Many-objective optimization and informed decision-making," *IEEE Transactions on Evolutionary Computation*, vol. 21, no.5 pp. 813–820, 2017.

[15] Z. He, G. G. Yen, J. Ding, "Knee based decision making and visualization in many-objective optimization," *IEEE Transactions on Evolutionary Computation*, vol. 25, no. 2 pp. 292–306, 2021.

[16] Y. H. Zhang and X. D. Wu, "Optimality and duality for multiobjective programming with generalized univexity," *Engineering Letters*, vol. 31, no.4, pp. 1561–1566, 2023.

[17] H. Y. Long, Z. X. Chen, H. Huang, L. X. Yu, Z. H. Li, J. Liu, and Y. Long, "Research on multi-objective optimization power flow of power system based on improved remora optimization algorithm," *Engineering Letters*, vol. 31, no.3, pp. 1191–1207, 2023.

[18] Z. Y. He, Y. N. Li, H. Li, and N. Xu, "Multi-objective optimization for online train trajectory planning with moving window method," *IAENG International Journal of Computer Science*, vol. 50, no.3, pp. 1074–1082, 2023.

[19] I. Das, "On characterizing the "knee" of the Pareto curve based on normal-boundary intersection," *Structural optimization*, vol. 18, no.2-3, pp. 107–115, 1999.

[20] H. Lu, "Simplified existence theorems on all fractional $[a, b]$-factors," *Discrete Applied Mathematics*, vol. 161, pp. 2075–2078, 2013.

[21] W. Gao, L. Liang, T. Xu, and J. Zhou, "Tight toughness condition for fractional (g, f, n)-critical graphs," *Journal of the Korean Mathematical Society*, vol. 51, no. 1, pp. 55–65, 2014.

Hainan Zhang received a B.E. degree in information and computing science from Liaoning University, Liaoning, China, in 2021. He is currently pursuing an M.E. degree in computer application technology at Yunnan Normal University, Kunming, China.

His current research interests include multitasking optimization, optimal optimization, and evolutionary algorithm.

Jianhou Gan received a Ph.D. degree in computational metallurgy from Kunming University of Science and Technology, Kunming, China, in 2016. Currently, he is a professor and doctoral supervisor at Yunnan Normal University. He was awarded the Yunnan Province "Ten Thousand Plan" industrial technology leading talent, young and middle-aged academic and technical leader. He is currently the Vice President of Yunnan Normal University, the vice director of the Key Laboratory of Educational Informatization for Nationalities, the Director of the Key Laboratory of Intelligent Education in Yunnan Province, and the leader of the innovation team in Yunnan Province.

His research interests include intelligent information processing, advanced database technology, education informatization, and intelligent education. He has undertaken more than 10 national scientific research projects such as the National Science and Technology Plan, the National Natural Science Foundation, and the National soft science project. He has published more than 80 papers, won 5 Yunnan Provincial Science and Technology Progress Awards, and authorized 12 national invention patents.

Juxiang Zhou received her Ph.D. degree in 2019 from the Dalian University of Technology, Dalian, China. Currently, she is an assistant research fellow at Yunnan Normal University.

Her research interests include Image and video understanding, intelligent image processing, and intelligent education. She has published more than 30 academic papers (including acceptance in international journals including IEEE Transactions on Cybernetics, Pattern Recognition, Information Science, International Journal of Machine Learning and Cybernetics, Multimedia Tools and Applications, and so on, authorized 9 national invention patents, and awarded the Yunnan Province Postdoctoral Excellence Award and the China Computer Society (CCF) Innovation Technology Award.

Wei Gao obtained a Ph.D. degree in the mathematical department at Soochow University, Suzhou, China in 2012. He is a professor in the School of Information Science and Technology, at Yunnan Normal University since 2019. He worked as a postdoctoral in the Department of Mathematics, Nanjing University from Jan. 2017 to Dec. 2018, and in the Department of Mathematics and Science Education, Harran University from Nov. 2019 to Oct. 2020.

His research interests are graph theory, statistical learning theory, discrete dynamic systems, nonlinear partial differential equations, artificial intelligence, etc. He is a committee member of the China Society of Industrial and Applied Mathematics (CSIAM) Graph Theory and Combinatorics with Applications Committee, and the chair of ISGTCTC 2018, ISTCS 2019, ISTCS 2022, and ISTCS 2023. He was rated in 2020 by Clarivate Analytics as a Highly-cited Researcher (Cross-Field), and by Stanford University as a World's Top 2% Scientist.